STUDY OF DENDRITE MORPHOLOGY, SYNAPSE ORGANIZATION, AND PROTEIN

LOCALIZATION IN DROSOPHILA EMBRYOS

by

RIDDHI ROY

(Under the Directions of Daichi Kamiyama and Oshri Avraham)

**ABSTRACT** 

Understanding how the neuronal circuitry functions at the cellular and molecular

levels is critical for unraveling deeper insights about neurological disorders. This study

investigates how genes linked to neurodevelopmental disorders affect dendritic architecture and

characterizes tools to study synaptic organization and protein localization. In this study, Trio and

Fmrl have been shown to affect various morphological aspects of dendrites in the aCC

motoneuron. A key challenge is the limited embryonic synapse markers, and it was addressed by

using epitope-tagged Rdl, a GABA subunit, which proved to be a reliable endogenous marker for

inhibitory synapses in embryos. Dlg, an excitatory synaptic marker, was overexpressed to mark

the postsynaptic structures. Protein localization can further the understanding of the genes and

their cellular functions, and using the split-GFP tool, we show that Nlg-4 localizes to postsynaptic

sites, and Nrx-1 is expressed in the presynaptic sites on the aCC motoneuron.

**INDEX WORDS:** 

dendrite, synapse, Nlg4, Nrx-1, neurodevelopmental disorders

# STUDY OF DENDRITE MORPHOLOGY, SYNAPSE ORGANIZATION, AND PROTEIN LOCALIZATION IN DROSOPHILA EMBRYOS

by

### RIDDHI ROY

B.Sc.., Nagpur University, India, 2020

A Thesis Submitted to the Graduate Faculty of The University of Georgia in Partial Fulfillment of the Requirements for the Degree

MASTER OF SCIENCE

ATHENS, GEORGIA

2025

© 2025

Riddhi Roy

All Rights Reserved

# STUDY OF DENDRITE MORPHOLOGY, SYNAPSE ORGANIZATION, AND PROTEIN LOCALIZATION IN DROSOPHILA EMBRYOS

by

### RIDDHI ROY

Major Professors: Daichi Kamiyama

Oshri Avraham

Committee: Jacek Gaertig

Vasant Muralidharan

Electronic Version Approved:

Ron Walcott Vice Provost for Graduate Education and Dean of the Graduate School The University of Georgia August 2025

## DEDICATION

To Sushrut, who taught me that there is always light at the end of the tunnel

#### **ACKNOWLEDGEMENTS**

This was a dream of an underconfident girl that turned into reality. I have a bunch of people to thank for it. I want to express my heartfelt gratitude for my PIs, Oshri and Daichi, for pushing me to do my absolute best and guiding me through these two years. Jacek and Vasant, I am very grateful for your suggestions and advice. My lab members, especially Melissa, Sam, Casey and Anthony, a big thank you for the suggestions, feedback, and moral support. I feel blessed to have my parents who have empathized with me, been my pillars of strength, and told me that I can achieve anything I dream of. A huge thanks to my amazing partner, Rishav Sen, who has seen me almost giving up to slowly pulling myself back up again, and has been extremely kind and supportive of me throughout this entire journey. To my best friends in India, Greece, and the US, who have inspired me to realize my entire potential, a big thank you. And last but not least, I want to thank myself for building the confidence, determination and resilience to never surrender and keep working hard. Always daydreamed about a thank you speech while receiving the Nobel Prize, but for now, this will do.

## TABLE OF CONTENTS

	Page
ACKNOWLEDGEMENTS	V
LIST OF TABLES	viii
LIST OF FIGURES	ix
CHAPTER	
1 INTRODUCTION	1
1.1. Study of the factors contributing to Neurodevelopmental disorders in humans	
through Drosophila	1
2 A COMPREHENSIVE PHENOTYPIC ANALYSIS AND CHARACTERIZATION	1 OF
DENDRITIC MORPHOLOGY, SYNAPTIC MARKERS AND PROTEIN	
LOCALIZATION	11
2.1. TRIO AND FMR1 MUTATIONS ALTER DENDRITIC MORPHOLOGY	11
2.2. CHARACTERIZING EXCITATORY AND INHIBITORY POSTSYNAPTIC	
MARKERS	22
2.3 SUBCELLULAR LOCALIZATION OF NLG4 AND NRX-1 USING SPLIT-GF	Ρ
SYSTEM	25
2.4. Discussion	30
2.5. Conclusion.	40
2.6. Future Directions	41
2.7 Materials and Methods	46

2.8. Supplementary figure	51
2.9. References	52

## LIST OF TABLES

		Page
Table 1:	Results from the statistical analysis of wild-type and mutant groups	19
Table 2:	Comparison of dendritic morphological changes in Trio and Fmr1 null mutants as	cross
previous	and current studies	34
Table 3:	Availability of mutants, MIMIC/CRIMIC lines, and neurodevelopmental disorder	rs
linked to	motor difficulties	43

## LIST OF FIGURES

Page
Figure 1: Wild-type embryo dendritic development in the ventral nerve cord10
Figure 2: Quantification methods of the dendrite morphological features
Figure 3: Quantification of dendritic morphological parameters in Trio and Fmr1 homozygous
null mutants
Figure 4: Subcellular localization of Rdl and Dlg at inhibitory and excitatory postsynaptic
sites
Figure 5: Study of subcellular localization of Nlg4 and Nrx-1 using the split-GFP system28
Figure 3S1: The number of dendrites for individual orders of branching

#### CHAPTER 1

#### INTRODUCTION

#### 1.1 Study of the factors contributing to Neurodevelopmental disorders in humans through

### **Drosophila**

Neurodevelopmental disorders (NDD) affect a huge population worldwide (>3% of children) [Parenti et al., 2020] and have a broad spectrum of associated diseases. They alter the motor, cognitive, and social functions of the affected individuals. NDDs range from Tourette Syndrome, which results in speech disorders, to Fragile X Syndrome, which causes intellectual disability(ID) and motor developmental delays. The Genome-Wide Association Studies (GWAS) integrated genes that are known to cause human diseases, and among them, 253 genes have been observed to cause NDDs. Despite consistent efforts to study these diseases, a lot is still unexplored and leads to conflicting opinions due to the complexities arising from studying these disorders across various animal models. The variations in phenotypes and severity in introduced mutations, gene regulation, and expression might confound the interpretations of the research findings.

The critical molecular pathways that have been determined to be involved in the various NDDs, as found through multiple studies, can be categorized into three groups: protein synthesis, synaptic signaling, and transcriptional regulation [Parenti et al., 2020]. Additionally, some NDDs arise from multiple factors, such as genetic disruptions and factors as well as environmental influences, whereas some develop from a monogenetic disruption, such as in Fragile X Syndrome [Jeibmann et al., 2009]. Hence, studying these various aspects can prove to be significantly critical in discovering more about the disorders and in turn fine-tuning the therapeutic targets for better clinical diagnosis and treatment options.

The fruit fly, *Drosophila melanogaster*, is an ideal model organism for several reasons, such as the ease of genetically manipulating the organism, the well-characterized genome, and the conservation of multiple fundamental biological pathways between humans and flies [Bagni et al.,2005; Avila et al., 2024; Jeibmann et al., 2009]. Additionally, there is a 75% homology of the human disease-causing genes in flies [Jeibmann et al., 2009]. Moreover, we have genetic tools such as the UAS-Gal4 system, which when combined with cell-specific promoters (see Figure 1(A)), target neuronal subpopulations to study specific gene expression [Parenti et al, 2020]. As seen in the schematic, in one parent fly, the Gal4 protein is under the regulation of a promoter (for example, eve). The other parent fly has the genomic region known as the UAS with the gene of interest located downstream of it. When these two flylines are crossed, the resulting progeny has the Gal4 protein, which binds to the UAS sequence. This binding activates the expression of the gene of interest, which can be fluorescent proteins, epitope tags, or used for ectopically expressing a gene. Hence, Drosophila has been a reliable resource for decades to unravel the biological mechanisms that play a critical role in nervous system development and the disorders related to it.

Neuronal connections are dependent on several factors and structures, such as the dendrites and axon terminals of neurons, neurotransmitters, synaptic vesicles, neurotransmitter receptors, and hundreds of other molecules facilitating the entire machinery. Dendrites are the fine processes of neurons and are on the receptive end of a synapse (see **Figure 1(B-D)**). The tree-like structures (arbors) that dendrites form have different morphologies and can provide useful insights about our understanding of the field. Our knowledge of dendritogenesis is limited due to the complicated arborization patterns and the minute size of the dendritic branches [Jan et al., 2010; Kamiyama et al., 2016]. Moreover, there are not sufficient available resources to resolve such fine structures due

to microscopic resolution limitations. Therefore, this understudied field of the underlying molecular mechanisms and factors that are responsible for maintaining dendrites needs more research, and over the last three decades, efforts have been made towards studying dendritogenesis in *Drosophila melanogaster*. Defects in dendritic and synaptic development might contribute to neurological and neurodevelopmental disorders such as Rett Syndrome, Fragile X Syndrome, and Autism Spectrum Disorders [Jan et al., 2010], which are also associated with motor deficits [Gatto and Broadie, 2011]. The Down Syndrome Cell Adhesion Molecule (DSCAM) is a widely studied gene due to its critical functions in neuronal development and its overexpression in individuals suffering from Down Syndrome, one of the common neurodevelopmental disorders. Several studies showed that the Dscam1 mutant impairs dendritic development [Inal et al.,2020; Hutchinson et al., 2014], and a null mutant in the early embryogenesis (15h after egg laying) phase displayed almost no dendritic outgrowth in the aCC motoneuron [Inal et al., 2020].

The dendritic morphology is studied in the anterior Corner Cell (aCC) motoneuron that innervates muscle 1(also called dorsal acute muscle 1) in Drosophila and is a well-characterized motoneuron. The aCC and RP2 are the only even-skipped (eve)-positive motoneurons, and they belong to the intersegmental nerve track (ISN) [Garces and Thor, 2006]. The aCC motoneuron has a stereotypical position, well-characterized lineage, and developmental timeline, which makes it a good candidate to study. Additionally, tools mentioned above, such as the UAS-Gal4 system, can be used to study the aCC motoneuron, where the Gal4 protein is under the control of the eve promoter and a reporter gene is placed downstream of the UAS region for driving expression. Upon the binding of the Gal4 protein to the UAS, the reporter gene, such as GFP or RFP, gets expressed in the cell subpopulation containing the Gal4 protein [Venken et al., 2011]. Importantly, this motoneuron has been a pioneer in studies related to axon development, dendrite formation,

and synapse targeting for the ease and convenience of studying it, thus providing more information related to it. This study focuses on the late embryogenesis stage, particularly the period of 18-20h after egg laying (AEL), which overlaps with the critical period (CP) of development. The CP is a sensitive developmental time point during which, if any manipulations are made in the organism, it becomes permanent and remains unaltered during the postembryonic stages, causing various behavioral and cellular phenotypes [Hunter et al., 2024]. A previous study suggested that manipulations during the 17.5 to 18.5 h AEL introduced delayed development in the locomotor circuitry of Drosophila whereas another study concluded that manipulations during the 17-19 h AEL window were sufficient to induce a seizure-like phenotype, which was observed as late as the third instar larval stage [Coulson et al., 2022]. NDDs such as Fragile X Syndrome, autism, schizophrenia, and epilepsy have been found to be strongly associated with unusual activity during CP [Hunter et al., 2024; Doll and Broadie, 2014]. Evidently, there are permanent changes in the neuronal circuitry, and it is important to study it at the molecular level to understand more about the plasticity of these structures during development and how they might contribute to neurodevelopmental disorders.

Another integral part of the neuronal circuitry is synaptic connections. Synapses are the regions where neurons communicate with each other, and neurotransmitters coordinate this entire process. Synapse formation and development play a crucial role in the neuronal circuitry, and changes in their organization or distribution might give rise to NDDs such as Autism Spectrum Disorder (ASD) and Intellectual Disability (ID) [Washbourne, 2015; Doll and Broadie, 2014]. The number of synapses changes with age due to the processes of synapse elimination and refinement (synapse pruning) that occur during childhood and adolescence periods in an individual's life [Doll and Broadie, 2014]. If these events are affected, then it impacts the excitatory/inhibitory(E/I) ratio

and balance in the brain, which translates to various NDDs. There are two main components that form a synapse: the presynaptic region, such as the axon of a neuron, and the postsynaptic region, like the dendrites of another neuron. The presynaptic machinery operates on the axon terminals to release neurotransmitters that bind to the receptors in the postsynaptic regions. Dendrites are sites where neurotransmitter receptors (NR) reside to receive the signals and complete synaptogenesis. However, not many postsynaptic markers have been developed since the excitatory and inhibitory receptors are not shared, and hence, each receptor needs to be labeled separately. Previous research studying synaptogenesis utilized overexpression markers to look at synaptic structures, due to the possibility of endogenous expression being too low or the ease of developing fusion constructs with fluorophores. Nevertheless, there are several caveats to that, such as producing ectopic or accumulation of synaptic sites in the cell soma. Moreover, it can also lead to the loss of the natural localization in the subcellular compartments [Parisi et al., 2023; Sanfilippo et al., 2024]. Due to such challenges, endogenous postsynaptic markers are even more limited in number but need development. Endogenous labeling is critical since it provides a more reliable and accurate representation of the subcellular locations of the various NR subunits in the postsynaptic sites at a particular stage of development and in a cell-specific manner [Sanfilippo et al., 2024].

The multi-level analysis study also investigates the subcellular localization of the proteins or genes involved with motor deficits in NDDs. Protein localization can provide valuable insights into the possible functions and roles that they play in the CNS. However, the challenges in studying the localization of proteins are: endogenous expression may be too low to be easily resolved, and achieving cell-type-specific labeling needs robust and sophisticated genetic tools. The split green fluorescent protein(split-GFP) strategy can address these issues. In this technique, GFP<sub>1-10</sub> is positioned downstream of a Gal4 line that drives GFP expression only in a subset of cells, and

GFP<sub>11</sub> is fused to a protein of interest, whose localization is being studied. The automatic reconstitution of the GFP<sub>1-10</sub> (a large N-terminal portion) and GFP<sub>11</sub> (a small C-terminal portion) fragments when they are in proximity results in a fluorescent signal. The fragments individually are unable to produce a signal, and hence, combining them allows for precise endogenous expression of protein localization in the cells expressing the Gal4 protein. It is even more helpful because one can observe the endogenous signal without the use of protein overexpression. Furthermore, the GFP<sub>11</sub> fragment can be amplified using multiple repeats and up to 7 times (often shown as GFP<sub>11x7</sub>), essentially indicating that a strong fluorescent signal is achievable. Minosmediated Integration Cassette (MiMIC) and CRISPR-mediated Integration Cassettes (CRIMIC) lines are tools that assist in the insertion of the GFP<sub>11</sub> fragment for tagging the protein of interest. MiMIC cassettes are inserted randomly into the genome, and when the GFP<sub>11</sub> is injected, it exchanges and gets located where the MiMIC cassette was originally before the exchange[Inal et al., 2024; Venken et al., 2011].

In this study, the dendritic morphological parameters studied to distinguish the phenotypes between wild-type and mutants are the total number of dendritic tips, branch distribution, total dendritic branch length, area of dendritic arborization, Sholl critical radius, and the distance between the center of the cell soma and the first primary dendritic outgrowth. Investigating multiple parameters can assist with categorizing the phenotypes based on their severity, where a less severe phenotype will result in significant deviations from the wild-type in a few morphological features instead of all. This comprehensive approach can help with the identification of core underlying pathways in scenarios that might be shared between genes, resulting in the determination of molecules working as a team whose disruption leads to NDDs.

Of the 253 NDD-related genes, 34 genes are found to be associated with motor deficits. In this study, we start with the phenotypic analysis of the Drosophila orthologs of Trio, also called trio in Drosophila and Fragile X mental retardation 1 (FMR1), also known as Fmr1 or dFmr1, to study the effects of their null mutations on dendritic morphology. Trio is a Guanine nucleotide exchange factor (GEF) and is shown to regulate the activity of Rho GTPases such as Rac in axon guidance and growth during embryogenesis. Trio was found to affect dendritic architecture in the da(dendrite-arborization) neurons that are part of the peripheral nervous system [Shivalkar and Giniger, 2012]. Fmr1 (Fragile X messenger ribonucleoprotein) encodes the FMRP(Fragile X Mental Retardation Protein) and loss-of-function mutations in the gene causes Fragile X Syndrome, a neurodevelopmental disorder in humans. Fmr1 plays a role in mRNA transport and the regulation of translation in dendrites and dendritic morphology [Bagni and Greenough, 2005].

Another objective is to study the synaptic organization of the NDD-associated genes using markers for neurotransmitter receptors or postsynaptic density proteins. To achieve this, we had to use multiple postsynaptic markers that would assist in studying both excitatory and inhibitory synaptic organization in the ventral nerve cord of the Drosophila embryo. We have utilized epitope-tagged NR subunits used in [Sanfilippo et al., 2024], such as V5 tagged-Rdl (Resistance to dieldrin) to successfully label the inhibitory synaptic sites endogenously. Additionally, the double recombinase system (see results and discussion) utilized to design the NR subunit lines assists with single neuron labeling, which is a significant benefit since it becomes increasingly difficult to distinguish between dendritic branching arising from two closely located neurons as development progresses due to complicated dendritic arborization. GABA (Gamma-Aminobutyric Acid) is a commonly found inhibitory neurotransmitter in vertebrates and invertebrates. Rdl encodes a GABA-gated chloride ion channel that is expressed highly in the central nervous system

(CNS) of the embryonic Drosophila. It starts to appear in the ventral nerve cord (VNC) of the Drosophila CNS at around stages 14-15 of embryogenesis (10.5-11.5h AEL), and it expresses everywhere in the CNS as it progresses further into the later stages of embryogenesis [Stilwell and ffrench-Constant, 1999]. Furthermore, the Drosophila ortholog of PSD-95, Discs large 1(Dlg1), is popularly used to label the excitatory synapses since it is a scaffolding protein present in the postsynaptic density along with neurotransmitter receptors and signaling molecules[Parisi et al., 2023]. We have utilized an overexpression Dlg flyline to preliminarily determine the possible sites of localization on the aCC motoneuron.

The third and last objective was to study the endogenous localization of NDD-related genes for meaningful insights regarding their cellular functions. Neuroligins(NLGN1-4) and Neurexin (NRXN1) are genes that are involved in NDDs such as Autism Spectrum Disorders(ASD), Intellectual Disability(ID), and Attention-Deficit/Hyperactivity Disorder (ADHD). Both of these genes encode cell adhesion molecules. There are four separate Neuroligin genes in Drosophila: Nlg1-4, and just a single Neurexin gene known as Nrx-1. A screening of the different isoforms of the Nlg using the split-GFP system revealed that Nlg4 had the strongest expression in the CNS. Neuroligins have been primarily shown to be involved in synaptic growth, synapse development, and regulating synaptic transmission. For the longest time, Nlg was thought of as a postsynaptic ligand of the presynaptic cell adhesion protein Nrx, but in vivo studies of Drosophila proved that Nlg4 specifically is a trans-synaptic protein that acts both presynaptically and postsynaptically at the neuromuscular junction (NMJ) [Zhang et al., 2017]. Neurexin has also been observed to be expressed in both presynaptic and postsynaptic regions at the NMJ and in the embryonic stages [Chen et al., 2010]. However, little is known about the roles in the cellular compartments in the

CNS apart from the NMJ and localization of both Nrx-1 and Nlg-4, and interestingly, both have been associated with motor deficits as part of the NDDs.

In summary, neurodevelopmental disorders are tightly linked to the disruption in dendrite morphology, synaptogenesis, and the correct neuronal protein localization. Despite years of research using both vertebrate and invertebrate models, the precise subcellular mechanisms that underlie such processes are poorly understood. In this thesis, I adopt a multi-level analysis approach to systematically examine the effects of null mutations on dendritic architecture, characterize postsynaptic markers to study synaptic organization and determine subcellular protein localization. These aspects are conceptualized as interconnected layers of a hierarchical system. This research framework allows to dissect how genetic perturbations can propagate through the dendritic processes and synapse organization to alter protein distributions, providing insights into neuropathology and neuronal development. The research objectives were achieved employing methods such as morphological quantification, endogenous receptor and single-neuron labelling, and split GFP-based localization to investigate the phenotypic effects of NDD-associated genes such as Trio, Fmr1, Nlg4, and Nrx-1, along with determining reliable markers such as Rdl and Dlg1.

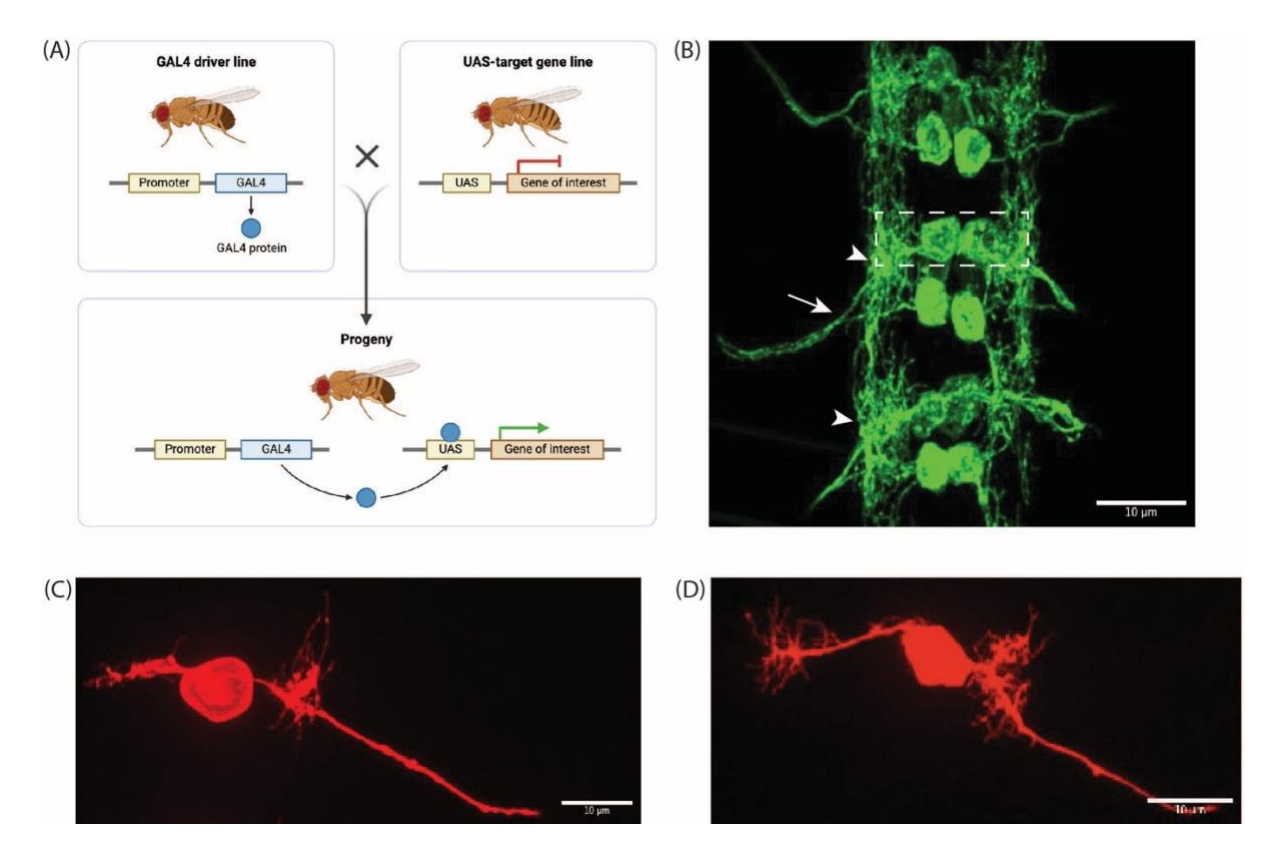


Figure 1: Wild-type embryo dendritic development in the ventral nerve cord (A) Schematic representation of the UAS-Gal4 system in Drosophila, a genetic tool to target a subpopulation of cells. (B) Representation of a Drosophila ventral nerve cord (shown are three abdominal segments) in an eve-Gal4 flyline, tagged with GFP. The aCC motoneuron is demarcated by the dotted rectangle in a single segment. The motoneuron below it is the other eve-positive motoneuron, RP2. The arrowheads point to the dendritic arborization of the aCC motoneuron, and the arrows point to the axon of the same motoneuron. Due to the Z-projection, the dendritic morphology is not well-resolved. (C) Dye-labeled aCC motoneuron at 16-17 h AEL. (D) Dye-labeled aCC motoneuron at 18-19 h AEL. Scale bar =10  $\mu$ m.

#### **CHAPTER 2**

A COMPREHENSIVE PHENOTYPIC ANALYSIS AND CHARACTERIZATION OF DENDRITIC MORPHOLOGY, SYNAPTIC MARKERS, AND PROTEIN LOCALIZATION Results:

#### 2.1 TRIO AND FMR1 MUTATIONS ALTER DENDRITIC MORPHOLOGY:

Previous studies have demonstrated that the aCC motoneuron is a good neuronal model in Drosophila to perform mutant phenotypic analysis on, as we have robust tools to visualize it, such as the UAS-Gal4 system. Several model systems have been used to demonstrate the effect of various genes known to cause neurodevelopmental disorders (NDDs) in humans, among which Drosophila is a popular choice. The short life cycle of Drosophila, ease of genetic manipulations, simple CNS structure, and availability of single-cell RNA sequencing data for various developmental stages are factors contributing towards it being an ideal model organism for studying cellular and molecular mechanisms. However, studying the dendritic features in the Drosophila motor system and in the late embryogenesis phase remained unexplored. In this study, Fmr1 and Trio were chosen as the genes of interest since they are known to cause NDDs in humans and additionally, show motor deficits as symptoms associated with the NDDs, which makes them good candidates to be studied in the motor system of the CNS. We use null homozygous mutations for both genes, acquired from the Bloomington Stock Center. Earlier studies on Trio and Fmr1 mostly focused on sensory neurons or the larval or pupal stages of the fruit fly. The later stages of embryogenesis (18-20 h AEL) also happen to overlap with the critical period of development, as

mentioned earlier. There has been no research focusing on the genetic mutations affecting the critical period of development that relates to dendritic morphology or synapse formation on dendrites. It is important to study the critical period since it has windows of heightened neuronal plasticity during which the brain is sensitive to experience-dependent changes that become "locked in" into the larval stages of development. Studying the potential morphological changes in the mutants in the embryonic stage can also help to investigate any behavioral changes in the later stages of development.

We used various manual and semi-manual methods to quantify and measure different morphological features of the dendrites. The methods to quantify the various dendritic parameters have been included in Figure 2(A-G). The various anatomical features of a wild-type aCC motoneuron are labeled in Figure 2(A). In Figure 2(B), the polygon method (see Materials and Methods for more details) is used to calculate the area coverage for the dendritic arborization. The dendritic branches have been manually traced using Fiji, as shown in Figure 2(C). The branches were traced, and their lengths were recorded. Upon measurement of all the dendrites, the lengths were summed to provide the total branch length (TBL). The Sholl analysis is demonstrated on the same motoneuron after thresholding it to increase the contrast with the background and eliminate background noise (see Figure 2(D)). The Sholl Critical Radius (SRC) was based on the maximum number of intersections recorded for a specific radius (denoted by concentric circles), as depicted by various colored dots. The schematic diagram in Figure 2(E) is representative of the various orders of dendritic branching (labeled and color-coded). Quantification of the orders of branching was performed as displayed in Figure 2(F), where each order of branching is annotated using numbers. Hence, 1 denotes primary branches, 2 denotes secondary branches, 3 denotes tertiary branches, so on and so forth. Each branching order is also denoted by a different colored dot for efficient counting and visualization purposes. **Figure 2(G)** represents how D, the distance between the first primary dendritic outgrowth and center of the cell body, was measured.

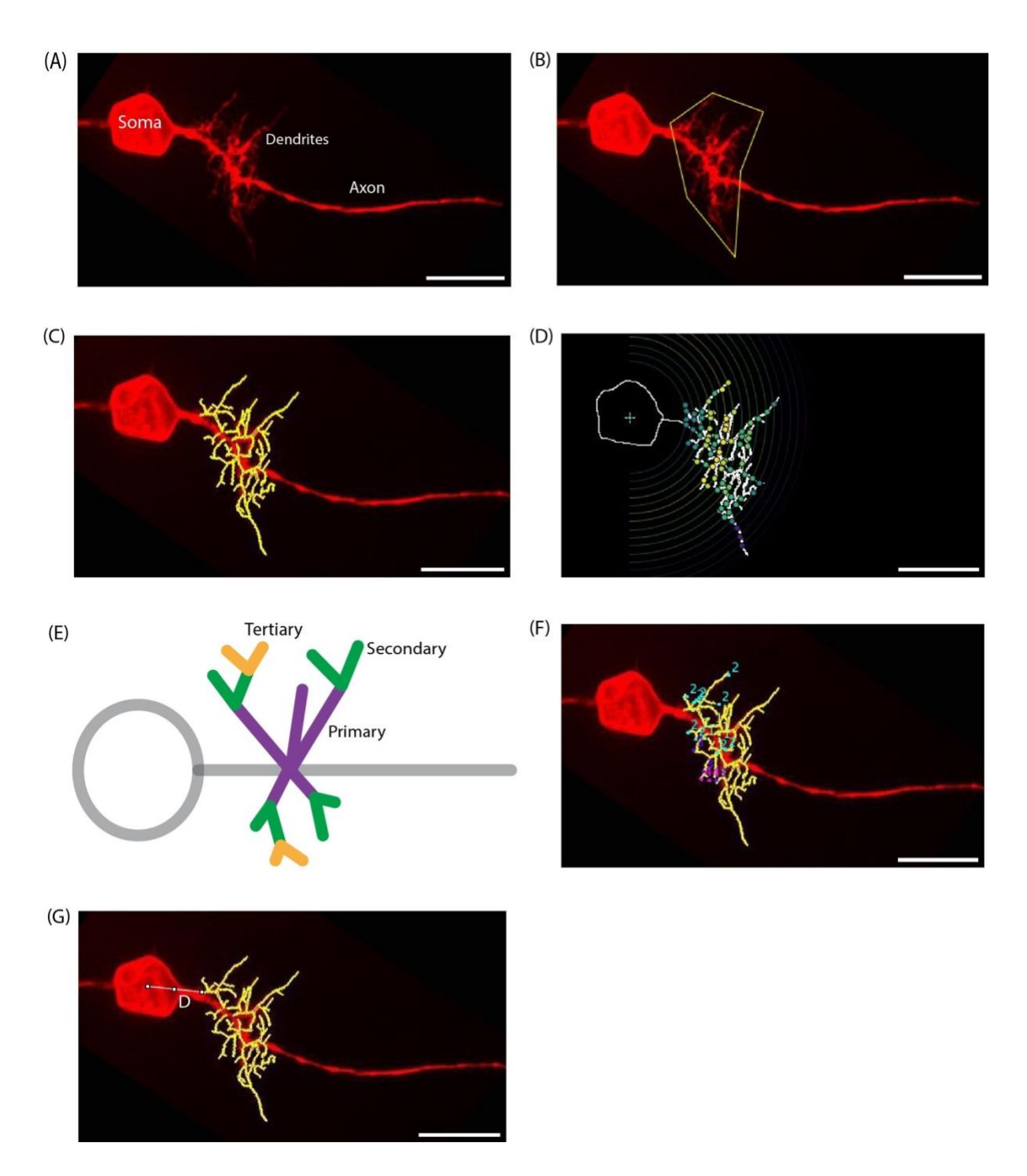


Figure 2: Quantification methods of the dendrite morphological features. All the images were

taken on the confocal microscope and at 100X magnification. (A) Representative image of dyelabeled wild-type (WT) aCC motoneuron. (B) The polygon method is used to calculate the area enclosing the dendritic arbor. (C) Manual dendrite tracing for measuring the total dendritic branch length. (D) Sholl analysis is performed by using concentric circles (shown here, half circles) and they are 1 µm apart from each other. (E) Schematic showing a motoneuron with cell soma and axon (in grey) and dendrites(colored). The orders of branching have been demarcated on the image. (F) The number of dendritic tips for each order of branching is counted and corresponds to the number accompanying the dots. (G) The method of quantification for D, the distance between the first primary dendrite and the center of the cell soma, has been demonstrated.

# 2.1.1. Loss of Trio alters dendritic morphology of the aCC motoneuron shows a severe phenotypic change:

A null mutant of Trio was used in this study. The flyline was created by introducing a chemical mutagen, ethyl methanesulfonate, to create a loss-of-function or null mutation. We decided to employ a retrograde dye-labeling technique utilizing lipophilic dyes, which associate with the hydrophobic membrane of the motoneuron, as shown in **Figure 3(A)**. This method was chosen over other available techniques for high spatial resolution of a single neuron and for better dendritic morphological visualization. We proceeded to quantify the number of dendritic tips irrespective of their order of branching to achieve a total count. As previously demonstrated in [Gatto and Broadie, 2011], the Trio null mutants were observed to have reduced dendritic branching and an increased average branch length in the sensory neurons of the Drosophila peripheral nervous system (PNS). Similarly, the Trio null homozygous mutant embryos were found to have a severe phenotype: the dendritic arborization was significantly reduced in size, and higher-order branching was affected. The total branch length of the dendrites was calculated, and

it was significantly lower in Trio (mean  $\pm$  SEM) as compared to the wild-type, as shown in **Figure 3(C).** The total number of dendritic tips was quantified. Upon quantification, it was found that it was significantly reduced compared to the wild-type group, as shown in Figure 3(D). To determine which order of branching had a significantly different number of dendrites between wild-type and mutant, primary and secondary order of dendrites were quantified individually. There were statistically significant differences in the numbers of primary, secondary, and tertiary dendrites between the wild-type and Trio mutant (Figure 3 Supplementary 1). The area covered by the dendritic arborization was found to be reduced in the Trio mutant as compared to the wildtype motoneurons (Figure 3(E)). Additionally, branch distribution with respect to the cell soma was quantified, but there was no significant difference in the distribution patterns between the wild-type and Trio mutants (Figure 3(F)). Once this was quantified, we wanted to see if the distribution of the dendritic arborization along the axon was altered. To achieve this, we quantified the length between the cell soma center and the first dendritic primary outgrowth (termed as D), irrespective of whether the dendritic outgrowth was above or below the axon. As observed in Figure 3(G), it was observed that the Trio mutants displayed a more distal placement of the first primary dendrite on the axon as compared to the wild-type. The Sholl critical radius was not of the Trio mutants was not vastly different from the control, as demonstrated statistically in Figure 3(H).

Together, trio homozygous null mutants demonstrated alterations in the various quantified morphological parameters and it indicates that the gene has multi-faceted functions assigned to it and interacts with a wide range of molecules to regulate various processes.

# 2.1.2. Loss of Fmr1 alters dendritic morphology of the aCC motoneuron and shows a moderately severe phenotypic change:

The Fmr1 study was performed using a null mutation of the gene generated through Delta2-3 transposase-mediated excision, a mutagenic approach that results in complete loss-of-function of the gene. As previously demonstrated in [Lee et al., 2003], Fmr1 affects dendritic branching and it was observed to result in increased higher-order branching in the dendritic arborization (DA) neurons in mutant Drosophila larvae. We wanted to see if it was DA neuron specific or showed similar phenotypes for other neuronal types, such as a motoneuron. Figure 3(B) below shows a representative image of a dye-labeled aCC motoneuron in a homozygous null Fmr1 mutant. Figure **3(C)** shows that the total branch length of the dendrites was calculated, and it is statistically significantly reduced (83.96±8.371 µm) as compared to the wild-type. The embryos were found to have no significant difference in total number of dendrites from those in the wild-type as seen in Figure 3(D). The number of dendrites was quantified according to their order of branching (primary, secondary, and tertiary), and there were no statistically significant differences for any order of branching between the wild-type and Fmr1 mutants (see Figure 3 Supplementary 1). The dendritic arborization area was significantly affected in the Fmr1 null mutants and decreased in size as opposed to in the wild-type (Figure 3(E)). The branching distribution (Figure 3(F)) did not show a significant difference from the wild-type. The distribution and positioning of the primary dendrite along the axon (termed as D), as seen in Figure 3(G) were similar (6.381  $\pm$  $0.3956 \mu m$ ) to the wild-type ( $5.882 \pm 0.3827 \mu m$ ). For both the Fmr1 mutant and the wild-type, the Sholl critical radius was not significantly distinct as evident in Figure 3(H).

Together, Fmr1 homozygous null mutants displayed altered morphological features, although not all features were significantly different from the wild-type. However, it is proof

of the multiple cellular and molecular roles of Fmr1 and how it is a key player in dendritic development and maintenance mechanisms.

The phenotypic analysis revealed that Trio and Fmr1 exhibit abnormal dendritic arborization characteristics. All the p-values, mean  $\pm$  SEM, and number of neurons(n) analyzed are mentioned in **Table 1** below.

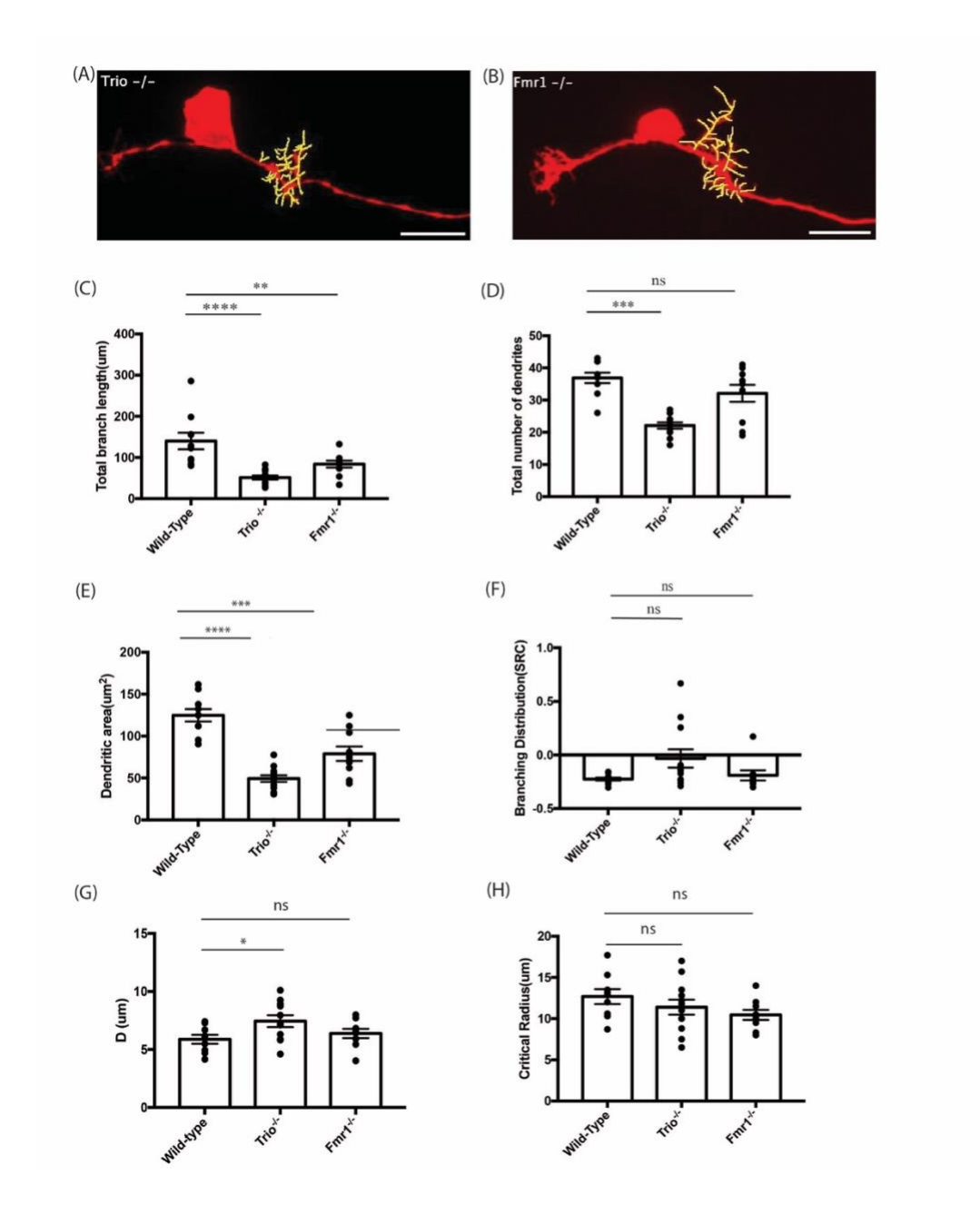


Figure 3: Quantification of dendrite morphological parameters in Trio and Fmr1 homozygous null mutants. All the images were taken on the confocal microscope and at 100X magnification. (A) Representative image of dye-labeled aCC motoneuron in Trio homozygous null mutant showing manually traced dendrites (in yellow). It displays a significantly reduced dendritic arbor. Scale bar =  $10 \mu m$ . (B) Representative image of dye-labeled aCC motoneuron in Fmr1 homozygous null mutant showing manually traced dendrites (in yellow). It does not

show a severely altered dendritic morphology as compared to WT. Scale bar =  $10 \mu m$ . (C) Bar graph showing total branch length (TBL, in  $\mu m$ ) and comparison between WT and the two mutant groups. (D) Bar graph showing the total number of dendritic tips and comparison between WT and the mutant groups. (E) Bar graph showing the area covered by the dendritic arborization (in  $\mu m^2$ ) in all groups. (F) Bar graph showing the branching distribution pattern and the spatial orientation with respect to the cell soma using the Sholl Regression Coefficient (SRC). (G) Quantification of the distance between the center of the cell soma and the first primary dendrite on the axon (termed as D, in  $\mu m$ ) and comparison of the distance between WT and mutant groups. (H) Critical radius calculated from the graph generated through Sholl analysis and plotted as a bar graph showing both WT and mutant groups. ns=not significant. Statistical significance is indicated as follows: p<0.05(\*), p<0.01(\*\*\*), p<0.001(\*\*\*\*).

TABLE 1: Results from the statistical analysis of the wild-type and mutant groups

Phenotypi c feature	Compariso n groups	Test	No. of neuro ns (WT)	No. of neurons( Trio)	No. of neurons( Fmr1)	Exact p value	Mean ± SEM
Total number of dendritic tips	WT vs Trio	Welch's t test	10	12		<0.0001	Trio=22.08 ±0.99; WT=36.9± 1.622
Total dendritic branch length	WT vs Trio	Welch's t test	10	12		0.0016	Trio=51.31 ±4.8 μm; WT=140.1 ±20.14 μm

Total dendritic field area	WT vs Trio	Welch's t test	10	12		<0.0001	Trio=49.31 $\pm$ 3.859 $\mu$ m <sup>2</sup> ; WT=124.8 $\pm$ 7.415 $\mu$ m <sup>2</sup>
Dendritic branching distributio n	WT vs Trio	Mann- Whitney	10	12		0.0591	Trio= - 0.03219±0. 0859; WT= - 0.2256±0.0 143
D	WT vs Trio	Welch's t test	9	11		0.0255	Trio=7.448 ± 0.5144 μm; WT= 5.882 ± 0.3827 μm
Sholl critical radius	WT vs Trio	Welch's t test	9	12		0.3265	Trio=11.4 $\pm 0.9007$ $\mu$ m; WT=12.69 $\pm 0.9079$ $\mu$ m
Total number of dendritic tips	WT vs Fmr1	Mann- Whitney	10		10	0.1587	Fmr1=32.1 ±2.618; WT=36.9± 1.622
Total dendritic branch length	WT vs Fmr1	Welch's t test	10		10	0.0244	Fmr1=83.9 6±8.371 μm; WT=140.1 ±20.14 μm
Total dendritic field area	WT vs Fmr1	Welch's t test	10		10	0.0008	Fmr1=78.9 $5 \pm 8.546$ $\mu$ m <sup>2</sup> ; WT=124.8 $\pm 7.415$ $\mu$ m <sup>2</sup>
Dendritic branching distributio n	WT vs Fmr1	Mann- Whitney	10		9	0.9682	Fmr1=- 0.1903 ± 0.0473; WT=- 0.2256±0.0 143

D	WT vs Fmr1	Welch' t test	9		9	0.3782	Fmr1=6.38 1 ± 0.3956 µm; WT=5.882 ± 0.3827 µm
Sholl critical radius	WT vs Fmr1	Welch's t test	9		9	0.0618	Fmr1=10.4 6 ± 0.6218 μm; WT= 12.69 ± 0.9079 μm
Total number of dendritic tips	WT vs Trio, WT vs Fmr1	Dunn's multiple compariso ns test	Same as above	Same as above	Same as above	0.0002, 0.3035	
Total dendritic branch length	WT vs Trio, WT vs Fmr1	Dunnett's multiple compariso ns test	Same as above	Same as above	Same as above	0.0001, 0.0071	
Total dendritic field area	WT vs Trio, WT vs Fmr1	Dunnett's multiple compariso ns test	Same as above	Same as above	Same as above	0.0001, 0.0001	
Dendritic branching distributio n	WT vs Trio, WT vs Fmr1	Dunn's multiple compariso ns test	Same as above	Same as above	Same as above	0.1081, >0.99	
D (Distance between centre of cell body and the first primary dendrite)	WT vs Trio WT vs Fmr1	Dunnett's multiple compariso ns test	Same as above	Same as above	Same as above	0.0361, 0.6721	
Sholl Critical Radius	WT vs Trio WT vs Fmr1	Dunnett's multiple compariso ns test	Same as above	Same as above	Same as above	0.4552, 0.1554	

### 2.2. CHARACTERIZING EXCITATORY AND INHIBITORY POSTSYNAPTIC MARKERS:

Numerous studies have investigated synaptic organization and transmission using neurotransmitter overexpression (OE) lines. However, these approaches cannot distinct between endogenous and ectopic expression levels, raising concerns regarding the physiological relevance of the observed patterns. Conversely, some proteins have limited expression at the embryonic stages, which compels the usage of OE flylines. In this study, we have utilized both endogenous and OE neurotransmitter receptors and postsynaptic density proteins to characterize reliable postsynaptic markers in the embryonic developmental stages.

#### 2.2.1. Labeling inhibitory synaptic sites on the dendrites using endogenous Rdl:

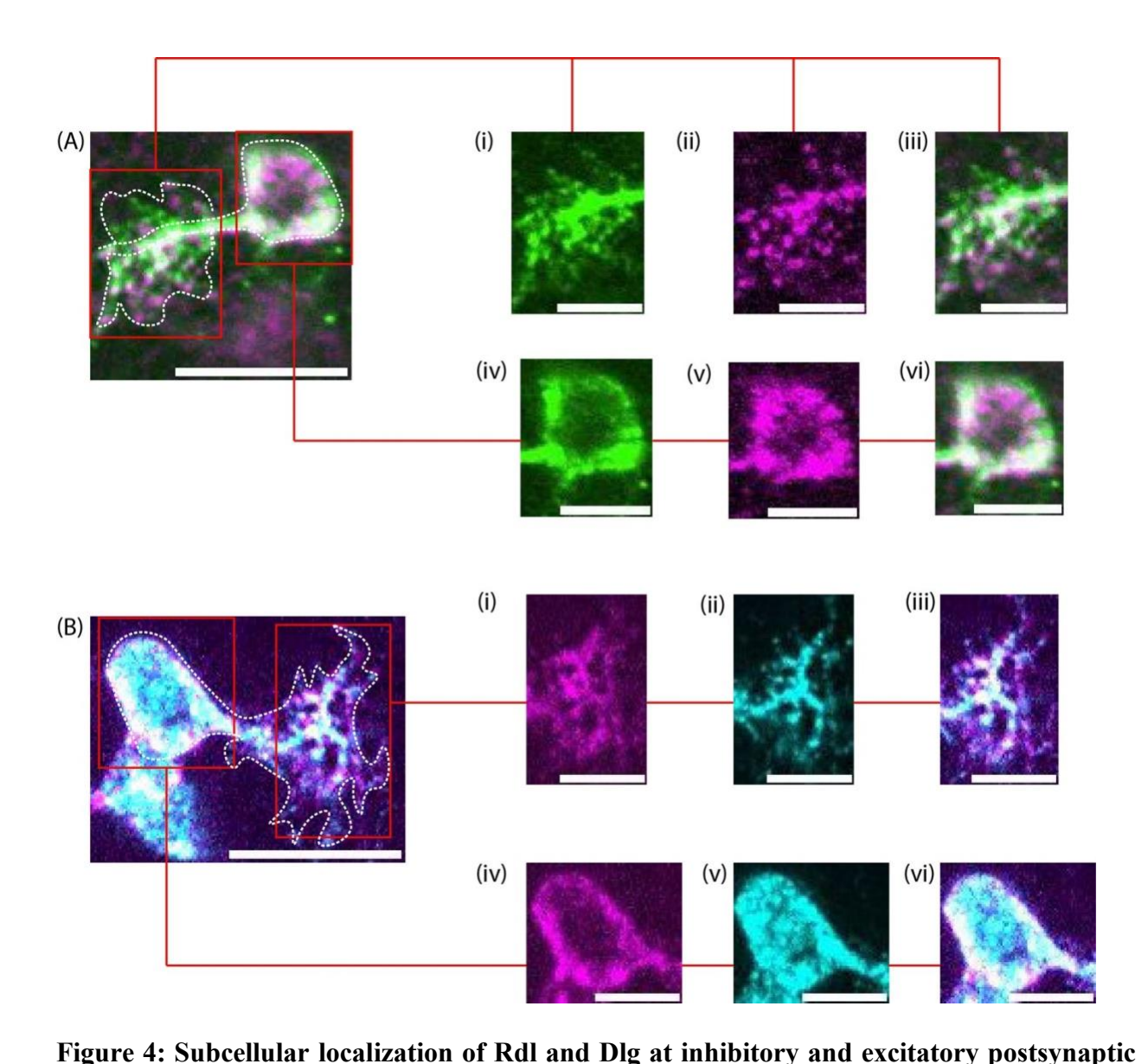
To visualize the Rdl protein, it was tagged with V5, and had a heat shock protein integrated into the Flippase (FLP) recombinase system. When the embryos are treated with heat shock, the Flippase gets activated and binds to the Flp Recombination Target (FRT) sites. These sites have a stop codon between them, which gets flanked off upon binding with activated Flippase. This flanking off drives the expression of genes, proteins or tags placed downstream of the FRT sites(here neuronal labeling with GFP, driven by eve promoter). The same mechanism operates in the KD recombinase (KDR) system, also placed downstream of the FLP system. In this instance, KDR drives specific NR subunit labeling as the construct has a V5 epitope tag downstream, which gets expressed when KDR binds to its target sites and flanks off the stop codon. Hence, upon heat shock treatment, dissection, and immunostaining against V5 and GFP (from eveGal4::tdGFP), the localization of Rdl was denoted through puncta formation and observed on the dendrites of the aCC motoneuron and on the axon, apart from the cell soma (shown in Figure 4(A)(i-vi)). The analyzed embryos did not display stochastic labeling, as was expected from the presence of the

heat-shock flippase system. Changes in factors such as the duration of heat shock (10 mins to 5 mins) and temperature (37°C to 28°C) were analyzed and tested, and yet optimal stochasticity was not achieved. The strong expression of Rdl was expected since it was one of the top differentially expressed NR subunit genes based on single-cell RNA sequencing data in embryos from a previous publication by [Seroka et al., 2022] showing the expression levels of various NR subunits, both excitatory and inhibitory, in the eve-positive motoneurons. Moreover, Rdl seems more concentrated on the aCC motoneuron and less on the RP2 motoneuron (not shown), which is located posterior to aCC and is also an eve-positive motoneuron.

To summarize, we used endogenous Rdl, a GABA receptor-subunit, to successfully label the inhibitory synaptic sites on the aCC motoneuron dendrites in the late embryonic stage of Drosophila. The aCC and RP2 motoneurons in all segments were labeled, and expression of Rdl receptors was uniform.

### 2.2.2. Labeling excitatory synaptic sites on the dendrites using overexpression Dlg:

Dlg is a scaffolding protein, widely used to mark the excitatory synapses and present in the postsynaptic density. We have utilized an overexpression Dlg flyline (unknown stock number) and introduced a yellow fluorescent protein (YFP) tag in it. In the OE line, a Tdtomato fluorophore was expressed under the control of a Gal4 driver specific to the eve-positive motoneuron, permitting membrane and neuronal morphology visualization. Upon dissection and immunostaining for YFP, Dlg OE was noted along the length of the axon and dendrites of the aCC motoneuron, besides being expressed in the cell soma (**Figure 4(B)(i-vi)**).



sites. (A) Representative image of the aCC motoneuron demonstrating Rdl(tagged with V5) subcellular localization in the cell soma, axon, and dendrites. Rdl, a GABA-A receptor subunit, is found at the inhibitory postsynaptic sites. Scale=10μm. (i) Immunostaining for GFP highlights the full dendritic arborization (green), enabling morphological visualization. (ii) Rdl distribution appears as puncta along the axonal and the dendritic compartments(magenta). (iii) Merged image of (i) and (ii) showing subcellular localization in the dendritic arborization along with the axonal

projection. (iv) The GFP signal (immunostained) defines the cell soma of the aCC

motoneuron(green). (v) Rdl localization within the cell soma, in addition to its distribution along the neurites(magenta). (vi) Merged image demonstrating the Rdl expression in the cell soma. Scale=5μm. (B) Representative image of the aCC motoneuron showing subcellular Dlg overexpression (OE). Dlg localizes to the excitatory postsynapses. Scale=10 μm. (i) The native signal of the membrane labeling the dendritic arborization(magenta). (ii) Punctated regions demarcating Dlg OE along the dendrites and the axon(cyan). (iii) Merged image demonstrating how the overexpression of Dlg shows up in the dendritic arbor. (iv) The membrane labeling the cell soma of the aCC motoneuron(magenta) (v) Dlg OE expression in the cell soma and along the axon(cyan) (vi) Merged channels showing both the membrane labeling and the overexpression of Dlg inside the cell soma and axon. Scale=5μm.

## 2.3. SUBCELLULAR LOCALIZATION OF NLG4 AND NRX-1 USING SPLIT-GFP SYSTEM:

Research during the past decade has demonstrated that cell adhesion molecules such as Nlg4 and Nrx-1 have played several roles in the maturation and transmission processes of synapses through various model organisms such as mice and Drosophila. For instance, loss of Nlg4 and Nrx-1 leads to a ruffled appearance on the trans-synaptic interface and, hence, causes sites of detachment, leading to a non-uniform interaction between the molecules and inefficient synapse transmission in Drosophila [Banerjee et al., 2016]. It was observed in Drosophila that a loss of Nlg4 resulted in an increase in the area of boutons in the active zones (AZ) [Zhang et al., 2017]. Another study in Drosophila showed that in the absence of Nrx-1, the size of the neuromuscular junction (NMJ) and the number of AZ per NMJ were significantly reduced [Chen et al., 2010]. Both these genes have been implicated in association with multiple NDDs and motor deficits [Nguyen et al., 2020]. These studies on Drosophila provided insights into the important roles of

these molecules in NDDs. However, a lot about the functions of these molecules in the motor system remains unexplored, and so does their spatial distribution and expression patterns, especially in the embryonic stages. Multiple studies in Drosophila melanogaster have employed the split-GFP system to achieve cell-type-specific expression and investigate the subcellular localization within the CNS [Inal et al., 2024; Kamiyama et al., 2021]. In this study, we have utilized the same tool to resolve the spatial localization patterns of both Nlg4 and Nrx-1 proteins within the Drosophila motor system. The eveGal4 flyline was used for driving GFP1-10 expression in the aCC motoneuron, and the available MiMIC(Minos-Mediated Integration Cassette) lines for Nlg4 and Nrx-1 were used and tagged with GFP11, which can be amplified up to 7 times (see Figure 5(A)). This can be achieved because the MiMIC lines contain two inverted attP (attachment phage) sites in a coding intron, which allows replacement of the DNA between those sites with the GFP11 fragment through Recombinase-Mediated Cassette Exchange (RMCE). This allows precise insertion of the GFP11 tag into the target genomic loci, facilitating the generation of split GFP-tagged proteins under native regulatory control. When both the GFP1-10 and GFP11 come close together, the GFP signal is reconstituted. CD4, a membrane marker, was tagged with tdTomato and was under the regulation of the eve promoter. It assisted in demarcating the membrane and delineating the neuronal morphology. To explore the subcellular localization of Nlg4, we immunostained for GFP. A similar approach was followed for Nrx-1. Both Nlg4 and Nrx-1 localize to different sites of the aCC motoneuron, corroborating the previous claims of Nlg4 playing a primary role in the postsynaptic terminal and Nrx-1 primarily being involved in the presynaptic terminal.

#### 2.3.1. Nlg4 localization in the aCC motoneuron cell soma and dendrites:

As mentioned previously, the membrane marker, CD4 tagged with TdTomato (expression was driven by eve promoter), was employed to visualize the morphology of the eve-positive motoneurons, enabling the spatial distribution patterns of Nlg4 relative to the neuronal membrane. To assess the localization, we performed immunostaining against reconstituted GFP using the anti-GFP Rabbit (monoclonal) primary antibody and anti-Rabbit 488 secondary antibody. Even though immunostaining would improve the resolution of dendrites, the overall morphology was evident due to sufficient fluorescent intensity for the assessment of localization. The Nlg4 was imaged in the 488 channel, and the membrane marker was imaged in the 547 channel (appears as cyan and magenta, respectively, in Figure 5(B)), exhibiting subcellular localization in both the soma as seen in Figure 5(B)(i-iii) and dendrites as seen in Figure 5(B)(iv-vi) of the WT aCC motoneuron. Notably, the dendritic enrichment varied across segments, with abdominal segments displaying a higher dendritic accumulation of Nlg4 relative to others (not shown). Furthermore, Nlg4 dominantly localizes to the proximal dendrites, close to the axonal projection. Therefore, it is noted that Nlg4 is localized to the postsynaptic sites.

## 2.3.2 Nrx-1 localization in the aCC motoneuron cell soma and axon:

Similar to Nlg4, CD4 was also employed as the membrane marker to delineate the neuronal morphological features. The immunostaining approach was analogous to that used for Nlg4, targeting reconstituted GFP. The membrane marker provided sufficient fluorescent intensity for visualization without immunostaining. The subcellular localization of Nrx-1 is seen in the cell soma and axon (presynaptic terminal of a synaptic site) of the WT aCC motoneuron (see **Figure 5C(i-vi)**). However, localization of the Nrx-1 was not evident on the dendrites upon analyzing the A2-A7 segments. Based on these findings, Nrx-1 has been concluded to localize to the presynaptic regions of the aCC motoneuron.

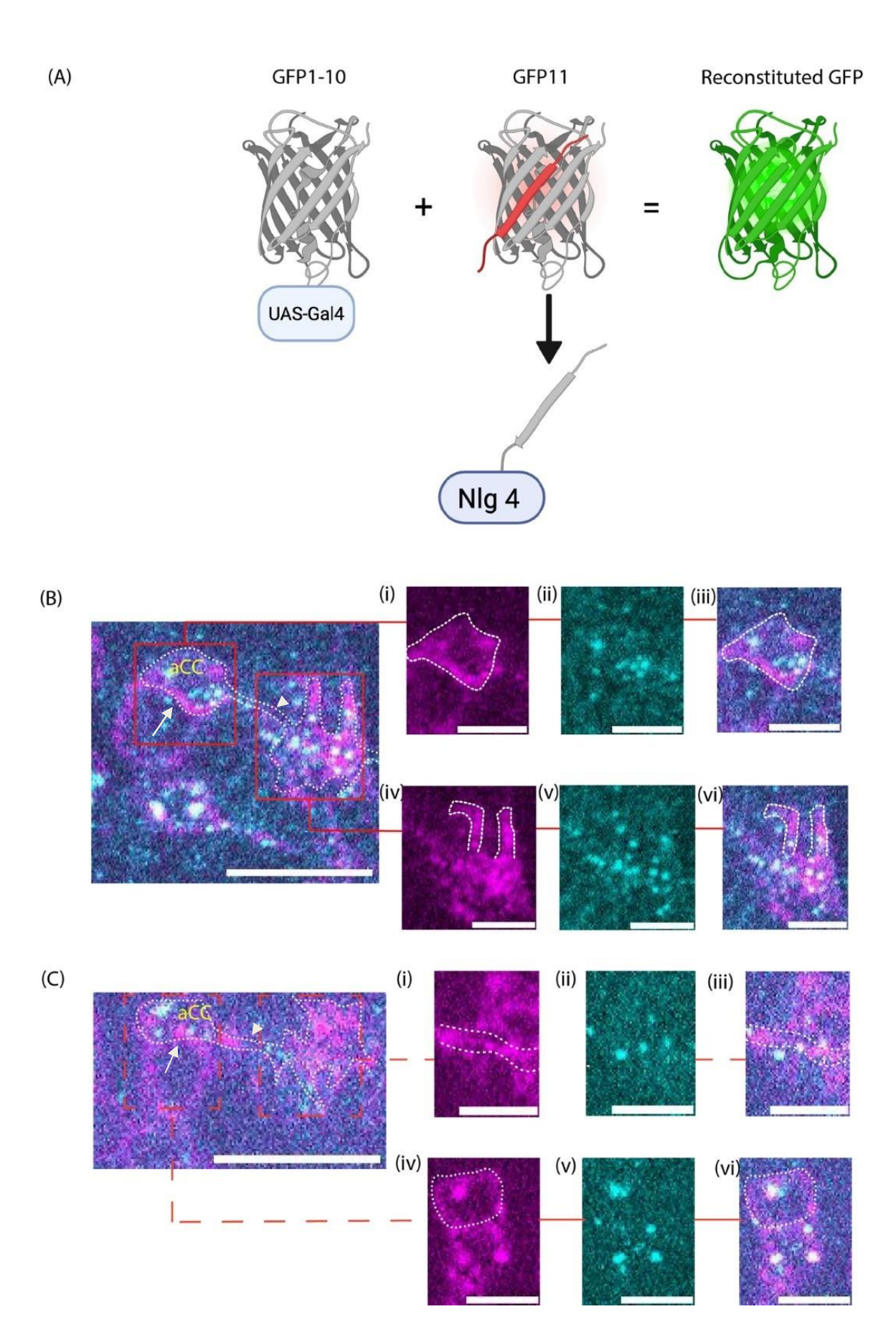


Figure 5: Study of subcellular localization of Nlg4 and Nrx-1 using the split-GFP systems. (A) Schematic diagram representing the principle underlying the split-GFP system. Membrane marker CD4 (magenta) and Nlg4 expression (cyan) were achieved through GFP reconstitution. The arrow points to the cell soma, and the arrowhead indicates the axon. (B) Representative image of Nlg4 expression in the CNS, and in the cell soma and dendrites of the aCC motoneuron. The boxes denote the areas that have been zoomed in on in the images labeled as (i) to (vi). Scale =10 µm. (i) The cell soma of aCC motoneuron. (ii) Nlg4 puncta in the cell soma region. (iii) Merged image showing the expression of Nlg4 in the cell soma of the aCC motoneuron. (iv) The dendrites of the aCC motoneuron, here the axonal outgrowth is visible, partially. (v) The expression of Nlg4 (as shown by the puncta) near the axon and on the dendrites of the aCC motoneuron. (vi) Merged image showing the expression of Nlg4 on the dendrites and near the axon. Scale for Figure 5B(i)-(vi) is 5 µm. (C) Representative image of Nrx-1 expression in the CNS, specifically in the cell soma (indicated by arrow) and axon (indicated by arrowhead) of the aCC motoneuron in the 18-20h AEL embryonic stage. The dotted boxes denote which areas have been zoomed in on in images labeled as (i) to (vi). The z-plane of the image differs from those in (i) to (vi) because this information was lacking in this plane. CD4 (magenta) and Nrx-1 expression(cyan) in the images. Scale =  $10 \mu m$ . (i) The dendritic arbor and a part of the axonal outgrowth. (ii) Nrx-1 puncta on the axon. (iii) Merged image demonstrating the localization of Nrx-1 in the axon. (iv) The cell soma of the aCC motoneuron. (v) The subcellular localization of Nrx-1 is denoted by the puncta. (vi) Merged image showing Nrx-1 localization in the cell soma of the motoneuron of interest, aCC. The z-planes of the cell soma and axonal localization are different from each other but belong to the same segment in the CNS. The scale for Figure 4C (i)-(vi) is 5 µm.

#### 2.4. Discussion:

# Trio and Fmr1 null mutants alter various morphological features of dendrites:

Drosophila is a great model system to probe into several diseases due to its simplistic organization and genetic and transgenic capabilities present for the organism. Previous studies in genes contributing to neurodevelopmental disorders (NDDs) are limited and have been investigated in the peripheral nervous system (PNS) or the central nervous system (CNS) of Drosophila adult, pupal, or larval stages. Moreover, the majority of the studies focused on the neuromuscular junction, mushroom bodies, or behavioral patterns [Doll and Broadie, 2014]. However, studying the diseases in the embryonic stage is crucial since it assists in determining the root causes and thus, helps in developing more targeted therapies. It can also help us in understanding at which point in development any phenotypic abnormalities can be detected and hence, allow for medical interventions at the earliest. As shown in studies of the influence of Trio on sensory neuron subclasses of the peripheral nervous system and in the third instar larval stage, mutations of Trio showed unusual dendritic branching. Additionally, Trio was found to impact the higher-order branching, which are actin-based as opposed to the primary dendrites, which are mainly composed of microtubules [Shivalkar and Giniger, 2012; Iyer et al., 2012]. Our observations of the dendritic branching of the aCC motoneuron in the CNS show a similar phenotype for the total number of dendrites. However, the quantification of each order of branching individually showed that the number of primary dendrites was also affected in the mutants, as were the higher-order branches, compared to the wild type (WT). This difference in observations might be due to differences in neuronal types (sensory vs. motor) as well as developmental stages (embryo vs. larva). The cytoskeletal composition of dendrites is mixed, having both actin and microtubules in the primary dendrites of motor neurons, which increases their dynamic nature and hence reduces stability.

Another possibility is that a mutation in Trio alters or shifts the balance of actin and microtubule compartmentalization. One of the factors contributing to the total dendritic branch length being reduced is the smaller number of dendritic branches. To determine if the dendritic length is regulated by Trio, it will require quantification of the average dendritic length. Additionally, the area coverage by the dendritic arborization in Trio mutants suggests that it was significantly lower than the WT, and the factors contributing to it are the decreases in both the number of dendritic tips as well as total branch length. The Sholl Regression Coefficient (SRC) is a measurement of the dendritic branching distribution patterns (see Materials and Methods). A more negative value of SRC implies a steeper decline in the number of intersections with increasing distance. The trio mutants did not show a significant difference in the spatial distribution of the dendrites as compared to the WT, but interestingly, they did show a wide variation in the coefficient values. The few positive values suggest that the trio mutants had more proximal dendritic branching, and there are very few to no distal intersections with increasing distance. This might be due to the variation in the values of the starting and ending radii specified for each sample to avoid inaccurate intersections (for example, the circle passing through the locations on the axon where there are no dendrites can add to the intersections). The other possibility, as mentioned above, is the instability of the dendrites in the Trio mutant, which results in a dynamic distribution pattern. Additionally, to determine if the radius of maximum number of intersections (Sholl critical radius) showed any alterations from the WT, we quantified it. However, upon analysis, it was found that there was no significant difference for this parameter. This further corroborates that the spatial distribution is overall unaffected in the mutants.

Another interesting finding was that the primary dendrites seemed to be shifted from their original positions along the axon (parameter termed as D) in the Trio mutants when the length

between the center of the cell body and the first primary dendritic branch was measured. An earlier study demonstrated that the Dscam1/Dock/Pak1 signaling pathway regulated the spatial extent of the aCC dendritogenesis site in Drosophila. It is also known that Cdc42, a small GTPase, regulates the timing of dendritic outgrowth during Drosophila embryogenesis. Working as a team, Cdc42 and Pak1 signaling pathway specifies the timing and region of dendrites [Kamiyama et al., 2015]. Moreover, Trio has been shown to regulate Rho family of GTPases such as Cdc42, Rac and Rho, all of which are key players for cytoskeletal dynamics, and a loss of Trio will downregulate them [Peng et al., 2010], which might affect the interactions with the downstream regulators or molecules from other pathways for dendritic positioning. A previous study in Drosophila found that the cell soma did shift from the midline in the RP2 motoneuron, adjacent to the aCC motoneuron in a Cdc42 gain-of-function mutant [Sánchez-Soriano et al., 2005]. Therefore, another possibility is that the cell body of the aCC motoneuron moved from its stereotypical position om the ventral nerve cord due to the change in cytoskeletal dynamics in the mutants. This might also be due to the critical roles that Trio plays in axon development and guidance, and a mutation reportedly leads to axonal stalling, guidance defects, and fasciculation defects [Awasaki et al., 2000]. However, it is not possible to scientifically explain more than this without further experimentation.

Previous research conducted on the Da (dendritic arborization) sensory neurons of Drosophila Fmr1 mutant third instar larvae showed that there was a significant increase in the number of terminal dendritic processes [Lee et al., 2003]. Another study demonstrated that there was an overelaboration defect in mushroom body neurons with an increase in the number of primary and secondary dendrites [Pan et al., 2004]. However, our quantification of the total dendritic tips was not significantly different from the WT. To determine if any specific order of

dendritic branching was affected, quantification was done separately. However, none of the branching orders was significantly different from wild-type, which contradicts the observation made for the sensory neurons of the PNS. This might indicate that the Fmr1 gene acts in a cellspecific manner. Moreover, this unaltered phenotype might be due to variations in developmental stages since previous research proved that an increase in the branch number was seen at the end of the first larval stage [Li et al., 2022]. Interestingly, the total branch length in the Fmr1 mutants was reduced, suggesting that Fmr1 might play a role in dendritic branch elongation. A loss of the Fmr1 gene might be playing a role in shortening the dendritic branches, resulting in an overall significant decrease in the total branch length. Due to the involvement of GTPases in dendritic morphology, it is likely that the GTPases might be playing a role in regulating dendritic length. Cdc42 was observed to be a key regulator of dendritic length in the neurons of the Drosophila visual system. It was believed that a loss-of-function of Cdc42 led to a significant increase in dendritic length [Scott et al., 2003]. However, it is difficult to say if it is the sole GTPase responsible for maintaining length, since studies in other model organisms, such as Xenopus, have concluded RhoA to be a regulator of dendritic length as well [Li, Van Aelst and Cline, 2000]. Furthermore, Pak1, which is a Cdc42 effector and has been previously mentioned for its role in dendritogenesis, interacts with FMR1 and FXR1 in mice and humans, respectively [Say et al., 2010]. The dendrite arbor area was significantly reduced, although the number of dendrites was similar to the wildtype. Thus, this also indicates reduced dendritic branch length. All observations from the previous research studies and the observations made during this study regarding changes in the morphology of the dendrites have been included in **Table 2** below.

Together, the data shows that Trio is key to the maintenance of dendritic characteristics like total branch length, area, number of tips, and possibly the placement of dendrites along the

axon. On the other hand, Fmr1 affected only the area and total branch length of the dendrites leading to a comparatively subtle phenotype.

TABLE 2: Comparison of dendritic morphological changes in Trio and Fmr1 null mutants across previous studies and this research study

Study citation	Observations	Similar or contrasting results found in this study
Shivalkar, M., & Giniger, E. (2012), Iyer, S. C. et al.(2012)	1. Trio heterozygote mutation affected higher-order dendritic branching and not the primary and secondary branches in Class I da sensory neurons at the larval stages.  2. The total number of dendrites was significantly reduced in Class IV da neurons.  3. Trio knockdown(RNAi) affected the dendrites both proximal and distal dendrites in Class III da neurons.	The total number of dendrites was significantly reduced dendrites in the Trio null mutant of aCC motoneuron in the late embryonic stage.  Affected both primary, secondary(proximal) and higher-order dendrites(distal).
Shivalkar, M., & Giniger, E. (2012), Iyer, S. C. et al.(2012)	Total dendritic length is overall significantly reduced in Trio knockdown and a Trio compound heterozygote in Class I and Class IV da neurons.	Total dendritic length is significantly reduced in Trio null mutants in the aCC motoneuron.
Shivalkar, M., & Giniger, E. (2012), Iyer, S. C. et al.(2012)	<ol> <li>Total dendritic coverage area of the Class I and Class IV da neurons got reduced in Trio knockdown.</li> <li>Total dendritic coverage area in Class IV da neurons did not get affected in Trio compound heterozygote.</li> </ol>	Total dendritic area of the aCC motoneuron got reduced in Trio null mutant.
Lee, A., Gao, F. B. et al. (2003), Pan, L. et al.(2004)	Number of terminal dendrites increased in Fmr1 loss-of-function mutation, in the da neurons at the larval stage.	There was no significant increase in the number of terminal dendrites as compared to the WT in the aCC motoneuron.

The number of secondary dendritic branches increased in	
the mushroom body neurons	
for the Fmr1 mutants.	

## Rdl and Dlg localized to inhibitory and excitatory postsynaptic sites:

A caveat in the tools to study synapse development and function is the lack of synaptic markers, especially for the structures involved in the postsynaptic terminal. Additionally, the markers available are not well-characterized in the embryonic stages of development in Drosophila due to the possibility of weaker expression patterns and difficulties in dissection. In this study, we aimed to label both inhibitory and excitatory synaptic sites through endogenous and overexpression labeling of various neurotransmitter receptor subunits.

The endogenous Rdl NR labeling was achieved by the use of a double recombinase system, where single neuron labeling, along with specific NR labeling, could be achieved [Sanfilippo et al., 2024]. It was observed that stochastic neuronal labeling was difficult and most, if not all, evepositive motoneurons were labeled. Achieving the stochasticity would have been beneficial in separating the dendritic arbor of the aCC motoneuron from the adjacent RP2 motoneuron. This might be due to the hypersensitivity and efficiency of the FLP construct, wherein even a small amount of the recombinase was capable of flanking the stop codon and driving Gal4 expression in the eve-positive motoneurons, like aCC and RP2. The FLP recombinase also regulates the activation of the KDR recombinase, which is placed downstream of Flp. The KDR recombinase system was employed to restrict the expression of Rdl receptors in the aCC and RP2 motoneurons. However, attempts to achieve sparse labeling were unsuccessful, likely due to the excessive or constitutive activation of the FLP recombinase, which led to uniform labeling of Rdl receptors on the motoneurons. One possibility of the stronger expression of Rdl in aCC motoneuron compared

to the RP2 motoneuron (not shown) might be owing to the more elaborate dendritic arborization of aCC- the higher number of dendrites provides more area for synaptic integration. The Rdl expression in the cell soma is possibly due to the translation of the protein, although we do not rule out the possibility of local protein translation in the axon or dendrites. The expression along the axonal outgrowth might be due to the transport of the protein to the dendrites post-manufacture in the cell soma. The other plausible explanation is that Rdl regulates presynaptic release in the axons. Similar observations were made in [Sanfilippo et al., 2024] where Rdl localized to both axon and dendrites in one of the mushroom body neurons. However, it partially contradicts the observations made in an earlier study, where Rdl was overexpressed and was tagged with an epitope tag, HA. They reported that they did not observe Rdl localization to the "primary neurites" along with presynaptic NMJ terminals, when overexpressed in all motoneurons [Sánchez-Soriano et al., 2005]. The phrase "primary neurites" has been used interchangeably with axonal processes, as interpreted from the data. This variation in observation might be a result of limitations in microscopic resolution or as a result of overexpression. Endogenous Rdl localization is also observed on the dendrites, as they are postsynaptic sites. Previous studies have demonstrated similar results where Rdl expression was found on the dendrites of MN5, a motoneuron innervating the flight muscle in Drosophila. It was also reported that Rdl preferentially localizes to the distal dendritic areas [Kuehn et al., 2013; Ryglewski et al., 2017]. However, we did not notice such an expression pattern on the dendrites of the aCC motoneuron. This difference in observations might arise due to different motoneurons being studied, different developmental stages, or even the functions associated with the particular motoneurons, which ultimately resulted in the variation of the distribution of synaptic sites along the dendrites, indicating different requirements of synaptic

integration. Together, these data suggest that endogenous Rdl is a reliable marker for Rdl-specific inhibitory postsynaptic sites.

To mark excitatory postsynapses on the aCC motoneuron, we used Dlg overexpression (OE). Dlg is used to label excitatory postsynapses not only because it is a well-characterized marker for excitatory synaptic sites [Harris et al., 2015; Sánchez-Soriano et al., 2005], but also because it is a general marker for these structures. This means that it has the benefit of labeling most, if not all, postsynapses in contrast to the different subunits of neurotransmitter receptors, which label only a subset of the postsynaptic structures [Sanfilippo et al., 2024]. Dlg expression in the cell soma is possibly due to it being the possible site of protein translation. The localization of Dlg to the dendritic arbors is consistent with previous studies, which showed that this protein belonged to the postsynaptic terminal. Although utilizing overexpression lines is not ideal, the preliminary data suggest that Dlg does localize to the postsynaptic sites on the dendrites of the aCC motoneuron. Although Dlg1 primarily functions at the postsynaptic terminal, genetic evidence suggests it may also play roles at presynaptic sites. Its sole well-characterized presynaptic function to date is the regulation of the muscle subsynaptic reticulum (SSR) presynaptically, where mutations in Dlg1 lead to a poorly developed and less complex SSR, and the phenotype could only be rescued after providing Dlg1 on the presynaptic membrane [Mendoza et al., 2003; Guan et al., 1996]. The axonal localization observed when Dlg is overexpressed might be pressing evidence that the protein also localizes to presynaptic sites and hence plays a role presynaptically in the Drosophila ventral nerve cord. Given that Dlg1 is a well-established marker of excitatory synapses, its colocalization with acetylcholine receptor subunits may serve as corroborative evidence to support its utility as a reliable postsynaptic marker in the future. However, the possibility of overexpression artifacts cannot be eliminated prior to looking at endogenous Dlg

expression under similar conditions. To summarize the results, Dlg OE localizes to both presynaptic and postsynaptic excitatory sites.

# Nlg4 and Nrx-1 act postsynaptically and presynaptically respectively in the aCC motoneuron:

Previous studies have explored the roles of Neuroligins (Nlg) and Neurexins (Nrx) in synapse transmission and maturation. It has been found that both the cell adhesion molecules are trans-synaptic. However, no research has yet looked into the cell-type-specific localization and expression in the embryonic stage of Drosophila and the motor system. It is important since this foundational data can assist in determining how protein localization patterns change from normal development and expand on their roles at the cellular and molecular levels, and eventually, provide useful insights about their relations to motor deficits in NDDs. The localization patterns for Nlg4 and Nrx-1 were uncovered using the split-GFP tool, and while the former localized to the dendrites, the latter localized to the axon of the aCC motoneuron, and below we discuss these observations.

It is evident that the cell soma expresses Nlg4 as suggested by the puncta formation, and the explanation for this is that there is a possibility that the protein translation occurs in the cytoplasm of the cell body. However, further experimentation is needed to rule out any possibility of local protein translation. The puncta are clearly seen on the dendrites and seem to be more concentrated in or near the branching points of the primary dendrites on the axons. The variation in the dendritic localization of Nlg4 across the abdominal segments in the ventral nerve cord (not shown) might be due to only immunostaining for the Nlg4 protein, but not the CD4 membrane marker. Due to the lack of immunostaining for the membrane marker, there is a possibility of underestimating the Nlg4 expression on the dendrites, and also because of limitations in image quality and resolution. The limitation could potentially be addressed by co-immunostaining for

both Nlg4 and the membrane marker to achieve improved structural resolution. However, this approach was not feasible in the present study as the available primary antibodies for both targets in the lab were raised in the same host species, precluding their simultaneous use without cross-reactivity. This observation confirms the presence of Nlg4 in the postsynaptic regions, as shown in previous studies [Nguyen et al., 2020; Zhang et al., 2017]. The localization of neuroligins (Nlg1, Nlg2, Nlg3) to the primary dendrites has been demonstrated in hippocampal neurons of mice, testing their association with FMRP. FMRP was observed to assist in synaptically regulating the local translation of Nlg1, Nlg2, and Nlg3 [Chmielewska et al., 2019]. However, this is the first study to show that Nlg4 also localizes to the proximal dendrites in the aCC motoneuron of Drosophila. This localization might reiterate the important role of Nlg4 in synapse maturation and transmission. Since the presence of Nlg4 in inhibitory synapses has been proven, it will be interesting to see if it colocalizes with Rdl. It is also yet to be seen or tested whether a null mutation of Nlg4 alters dendritic morphology and the spatial distribution of synapses along the dendritic branches.

The absence of Nrx-1 from the dendrites and its presence on the axon (in **Figure 5(C)(i-iii)**) corroborates the primary role of this cell adhesion molecule in the presynaptic zone for efficient synaptic transmission and synapse maturation [Zeng et al., 2007; Krueger et al., 2012; Chen et al., 2010]. Furthermore, expression of Nrx-1 in the cell soma (in **Figure 5C(iv-vi)**) suggests that it is possibly the translation site of the protein. However, unless both the membrane and Nrx-1 are co-immunostained, there is a possibility of undermining the expression and its presence on the dendrites. Additionally, to make further scientific claims, the phenotype should be examined in Nrx-1 null mutants. Without this, it does not rule out the possibility of Nrx-1 being involved in morphological alterations in dendrites or synaptic organization on the dendrites. Often,

there are multiple key players making such events possible, and the deficiency in just one of the team players can totally alter a cellular event.

Together, the data suggest that the sites of localization differ between Nlg4 and Nrx-1 in the WT aCC motoneuron, and this suggests differences in their cellular and molecular functions and roles. Nlg4 is primarily localized to postsynaptic regions such as dendrites along with the cell soma, whereas expression of Nrx-1 was observed in presynaptic regions of the aCC motoneurons, such as the axon, besides the cell soma.

#### 2.5. Conclusion

It is critical to look at the different angles of the neuronal circuitry to unravel the underlying mechanisms of neurodevelopmental disorders, especially at the embryonic level and the critical period of development. The previous studies investigating the mechanisms underlying NDDs have predominantly focused on the PNS and larval stages of Drosophila development, primarily due to the ease of anatomical accessibility and visualization at these stages. However, to achieve deeper insights that are directly translatable to motor deficits observed in NDDs, it is crucial to examine these processes within the Drosophila motor system itself. Our study found that both Trio and Fmr1 are genes controlling various morphological aspects of dendrites in the aCC motoneuron at the embryonic level. Through our research, we have established the pipelines to study synapse organization by the characterization of postsynaptic markers using endogenous Rdl and Dlg overexpression in the aCC motoneuron in the late embryonic(18-20h AEL) period in Drosophila. The split-GFP tool has been utilized in the aCC motoneuron to determine the endogenous localization sites of the motor-deficit-related genes and, therefore, provide meaningful insights about their molecular and cellular functions. An abnormal dendritic

morphology, altered synaptic organization, or mislocalized protein expression can form the basis for NDDs.

#### 2.6. Future Directions

34 genes have been identified to be associated with abnormal motor responses, gross motor development, and motor deficits such as locomotion or gait disorders, as shown in the table below. 26 out of the 34 genes have amorphic(or null) or hypomorphic mutants available (such as Trio and Fmr1), and 15 out of the 34 genes have MiMIC/CRIMIC lines available, which can be used for studying protein localization as demonstrated through Nlg-4. The localization can be categorized by the sites in the VNC where these proteins are found (for instance, in dendrites, axons, and synapses) to prioritize the genes that might be involved in dendrite and synapse development.

This study has demonstrated that Trio and Fmr1 are genes required for proper dendritic morphology, and null mutations of these genes result in alterations in all or some of the quantified parameters, which are the number of dendritic branches, dendritic initiation site along the axon, total dendritic branch length and total area covered by dendritic arborization. The phenotypic analyses will allow comparison among the mutations of all 15 gene orthologs and help in determining similarities and differences among the genes. The observations might help to identify common or shared pathways and downstream molecules and add to the understanding of NDDs.

An automatic pipeline for dendritic morphology quantification can be devised using AI technology, and better-quality images can be obtained using super-resolution microscopy. Furthermore, future experiments can explore which Rho GTPases or effectors (such as Pak1) interact with Trio and Fmr1 and which other downstream molecules or pathways are crucial in the formation of dendrites in motoneurons.

A lack of reliable markers for synapses has been a long-standing challenge in the field, and it was essential to characterize neurotransmitter receptors or associated proteins that could selectively delineate synaptic regions along the dendritic arbors. The excitatory and inhibitory synaptic markers (Dlg and Rdl, respectively) have been determined to successfully mark the postsynaptic sites on the dendrites in the wild-type embryos and can be extended to the mutants of the Drosophila orthologs of genes leading to motor deficits in NDDs.

Therefore, an automatic pipeline can be used for synaptic quantification (detecting puncta in the dendritic regions). Additionally, the distribution of the synapses on the dendrites can be measured using software tools such as Icy, which can perform Ripley's K analysis. This distribution pattern (clustering, even, or random) can indicate if a specific distribution pattern indicates a synaptic versus a non-synaptic region on the dendritic branches. Additionally, it can serve as a parameter to distinguish between altered distribution patterns between wild-type and mutants. Moreover, performing behavioral assays in the mutants of the gene orthologs would enable a direct correlation between structural alterations and motor functions, thereby facilitating the classification of specific motor phenotypes, if present.

The protein localization studies of Nlg4 and Nrx-1 have been successful in determining the possible sites of expression on the aCC motoneuron. However, it is equally important to explore whether the localization will change in mutant backgrounds so that a direct relationship between inefficient synapse transmission or maturation and abnormal motor responses can be established. Furthermore, all the other available MiMIC and CRIMIC lines for these genes can follow a similar experimental approach where normal localization patterns are noted before testing them in amoprhic or hypomorphic mutants and recording any abnormal phenotypes.

Together, the experiments will be fundamental to shed light on the shared or common mechanisms or pathways that underlie the pathophysiology of NDDs and hence, assist in determining potential therapeutic targets and devising diagnostic strategies for medical intervention as early as the embryonic or fetal stages.

TABLE 3: Availability of mutants, MIMIC/CRIMIC lines, and neurodevelopmental disorders linked to motor difficulties

Human NDD	Drosophila	MIMIC/CRIM	Mutant	Neurodevelop
genes	ortholog	IC lines	availability	mental disorders
SPAST	Spas	CRIMIC #79252	amorphic	Hereditary Spastic Paraplegia
KIF11	Klp61F		No	Microencephaly with or without chorioetinopath y, lymphedema, intellectual disability
DYNC1H1	Dhc64C	CRIMIC #78869	loss of function, amorphic, hypomorphic	Spinal muscular atrophy with lower extremity predominance
STXBP1	Rop	CRIMIC	amorphic, hypomorphic	Early Infantile Epileptic Encephalopathy -4 (EIEE4)
GRIN2A, GRIN2B	Nmdar2		No	Epileptic Encephalopathy with Motor Deficits
MECP2	MBD-like		No	Rett Syndrome
UBE3A	ube3a		loss of function, amorphic	Angelman Syndrome
PTEN	pten		loss of function, amorphic, hypomorphic	Autism Spectrum Disorders

				having motor deficits
SCN1A, SCN2A	NaCP60E	MIMIC #60210	loss of function	Dravet syndrome (severe epilepsy with movement impairment)
TSC1	Tsc1		No	Tuberous sclerosis complex
NLGN4X	Nlg3, Nlg4, Nlg1	MIMIC #76134,59786,6 7439,60206,602 46	amorphic	Autism Spectrum Disorders
ATP1A2	ATP alpha		hypomorphic, loss of function, gain of function	Familial hemiplegic migraine, Alternating hemiplagia of childhood
GABRB2/GAB	Lcch3, Rdl	MIMIC(Rdl	amorphic for	encephalopathie
RB3/GABRA1	GY O2	#59796)	Rdl	s and epilepsy
KCNT1	SLO2	MIMIC #63152	No	Epilepsy
NF1	Nf1	CRIMIC	loss of function	Neurofibromato sis type 1
PURA	Pur-alpha		No	PURA syndrome
SLC2A1	Glut1		No	Glut1 deficiency syndrome
SYNGAP1	raskol		No	Intellectual Disability, Autism Spectrum Disorder
DSCAM	Dscam4, Dscam2, Dscam1, Dscam3	MIMIC #60155,61758, CRIMIC	amorphic	Down syndrome, autism spectrum disorders
DYRK1A	mnb	MIMIC #66769, CRIMIC	Hypomorphic	Down syndrome, Autism spectrum disorders

FOXP1/FOXP2	FoxP	CRIMIC	hypomorphic, amorphic	Autism Spectrum
			_	Disorders
MAGEL2	MAGE		amorphic	Schaaf-Yang
				Syndrome,
				Autism
				spectrum
				disorders
CACNA1A	cac	MIMIC #67444,	hypomorphic,	spilepsy,
		CRIMIC	loss of function	episodic ataxia,
				autism spectrum
				disorder
CACNA1C	cac-alpha1d		amorphic	gain-of-function
				leads to
				Timothy
				Syndrome
CACNA1E	cac	MIMIC #67444	hypomorphic,	epileptic
			loss of function	encephalophath
				у
CASK	CASK	MIMIC	Hypomorphic	pontocerebellar
		#59768,76631		hypoplasia
CAMK2A/CA	CAMKII	MIMIC #93667,	loss of function	severe
MK2B		97756		intellectual
				disability
CHD7	kis	MIMIC #76131,	loss of function	CHARGE
		CRIMIC		syndrome
CHD8	kis	MIMIC #76131,	loss of function	Autism
		CRIMIC		Spectrum
				Disorders
CTNNB1	arm	MIMIC #60561,	amorphic,	CTNNB1
		66903	hypomorphic	syndrome
NRXN1	Nrx-1	MIMIC	amorphic	Autism
		#67489		Spectrum
				Disorders,
				ADHD
TRIO	trio	MIMIC #59808,	amorphic,	mild to severe
		76752	hypomorphic	intellectual
				disability,
				autism spectrum
				disorders
FMR1	Fmr1	MIMIC #67486	amorphic,	Fragile X
			hypomorphic	Syndrome

#### 2.7. Materials and Methods:

#### Fly strains:

For mutant analyses, trio (RRID:BDSC\_9129) and Fmr1(RRID:BDSC\_6930) were obtained from Bloomington Stock Center. The other lines that were obtained from the Bloomington Stock Center were RRID:BDSC\_39692, RRID:BDSC\_602277, RRID:BDSC\_602270, RRID:BDSC\_44304, RRID:BDSC\_55467, RRID:BDSC\_35837 and RRID:BDSC\_7473.

# **Embryonic Collection and Dissection:**

The embryos were collected on grape juice-coated agar plates at 25°C for 2 hours and then plates were changed. The collected embryos were kept at 25°C till they aged to 18-20 h AEL. Embryonic dissection was done in a similar way, as shown by [Inal et al., 2020] with slight variations. The embryos were dissected on plastic microscopic slides, and a UV Glue kit for the late-stage embryos (18-20 h AEL). Once the embryos were dragged out from the vitelline membrane, they were placed into the glue and UV light was used to solidify the glue so that the ventral surface of the embryos was stuck and then dissection followed.

#### **Immunohistochemistry:**

Dissected embryos were fixed with 1ml of 4% paraformaldehyde (PFA) for 5 mins and washed thrice with 1x PBS. 100-200 µl of TBS (49.5 ml of 1X PBS, 500 ul of 0.01% Triton X-100) was used to wash the samples for 5 mins thrice for membrane permeabilization before blocking the samples with TBSB (0.1% Triton X-100+ 1X PBS+ 0.06% BSA) for 1h at room temperature. For dropping the dye on the aCC motoneuron, the samples were incubated with Goat anti-HRP conjugated to Alexa Fluor 488 for visualization under the fluorescence microscope. The following primary antibodies used were anti-GFP monoclonal (Rabbit, 1:500; Thermo Fisher Scientific #G10362), and anti-V5(Rabbit, 1:300). The following secondary antibodies used were Alexa Fluor

488(Rabbit, 1:500; Thermo Fisher Scientific # A21206), Alexa Fluor 647(Rabbit, 1:500; # A31573) and anti-HRP conjugated to Alexa Fluor 488(Jackson ImmunoResearch #123-545-021).

## **Neurotransmitter receptor visualization:**

For Rdl, the embryos were collected for 2 hours at 25°C on grape juice-coated agar plates streaked with yeast. After collection, the embryos were heat-shocked for 10 minutes at 37°C and kept at 25°C until dissection at the 18-20 h AEL stage. The Rdl construct was tagged with an epitope tag(such as V5) and immunostained for imaging with a confocal microscope. The endogenous Dlg flyline had an FLP recombinase system to regulate the stochastic labeling in the eve-positive motoneurons.

#### Fluorescence imaging:

The embryos were screened for homozygous mutants for both the trio and fmr1 lines. Fillet embryos carrying no green fluorescent protein indicated homozygous mutation for both lines. The embryo screening was done using an inverted fluorescence microscope with a 10x 0.25 NA air objective lens (Nikon). The dye-labeled aCC motoneurons were captured via confocal microscopy using the 100x 1.45NA oil immersion objective. The microscope was attached to the Dragonfly Spinning disk confocal unit. There were three excitation lasers (488 nm, 561 nm and 647 nm) that were coupled to a multimode filter passing through the Borealis unit (Andor). A Dragonfly laser dichroic mirror and three bandpass filters were placed in the imaging path. Images were recorded using the iXon Andor camera, which is an electron-multiplying charge-coupled device camera. The confocal stacks acquired were 0.5 µm z-steps.

## **Measurement of dendritic parameters:**

a. **Dendritic field area:** The dendritic arborization area was measured using the polygon method as previously shown in [Shivalkar and Giniger, 2012; Grueber et al., 2002]. The

- most distant/longest dendritic tips are joined using the polygon selection tool in Fiji. Once the outline is made, the area enclosing the entire dendritic arborization area is measured.
- b. **Total number of dendritic tips:** The number of dendritic tips was counted using the cell counter plugin in Fiji. The primary, secondary, and tertiary branches were counted using different colors for successful annotation, and the numbers were displayed in a table format through the plugin. All the numbers were summed up to get the total number of dendritic tips.
- c. **Total dendritic branch length:** The dendritic branches were traced using the freehand tool on Fiji for accurate length measurements and each tracing was saved on the ROI manager. The z projection of the image was used as a reference when tracing the dendrites plane by plane for accuracy. The lengths were measured and stored as an Excel file and summed up to get the total dendritic branch length of each neuron.
- d. **Dendritic branch distribution:** The Neuroanatomy plugin's Sholl analysis function on Fiji was used for analyzing the images and recording the number of intersections per radius. The log value of N/S (intersections/area) is also provided through Sholl analysis, and those values are plotted against r (radial distance) to determine the Sholl Regression Coefficient (SRC). It was done in the same way as described in [Stanko et al., 2015]. The formula for calculating the Sholl Regression Coefficient is: log N(r)= k.r+b, where,
  - N= number of intersections, r= radius, k= regression coefficient(slope), b=intercept.
- e. **Dendritic outgrowth along the axonal projection:** The line tool in Fiji was used for quantifying the distance between the centre of the cell soma and the first primary dendritic branch growing out from the axon of the aCC motoneuron.

f. **Sholl critical radius:** The Sholl analysis function creates a graph mapping the number of intersections against the range of the radius values. The radius displaying the maximum number of intersections was noted to be the Sholl Critical Radius, representing the peak point of dendritic complexity relative to the cell soma.

All the quantifications and measurements were stored on Microsoft Excel.

# Dye labeling:

Dye labeling was done according to the protocol described in [Inal et al., 2020]. The embryos were immunostained using an anti-HRP antibody conjugated with a secondary antibody. This enabled to define the neuronal membrane under the fluorescence microscope and aided in dropping the dye on the target motoneuron. D labeling (Thermo Fisher Scientific) was performed in embryos at 18-20h AEL in both wild-type and mutant backgrounds for phenotypic analysis of dendritic processes. The variation of motoneuronal structure and dendritic morphology is due to various abdominal segments in which the aCC motoneurons were labeled.

## **Statistical analyses:**

Statistical analyses were performed using GraphPad Prism 7.0. All datasets were evaluated for normality using the Shapiro-Wilk's Test and unpaired parametric Welsh's t-test was used when the data distribution was normal and the non-parametric Mann Whitney U test for non-normal data distribution. For comparison between the wild-type and the two mutants together, one-way ANOVA or Kruskal Wallis tests (dependent on parametric or nonparametric data) were performed for each of the parameters. Error bars are shown as the standard error of the mean (SEM) in the figures.

#### **Software tools:**

The quantification of all the dendrite morphological parameters was performed using various Fiji plugins. Microsoft Excel was used for the storage of all the measurements and data from the analysis. GraphPad Prism helped perform all statistical analyses. Figures and schematics were developed using Adobe Illustrator, Adobe Photoshop, and BioRender.

# 2.8. Supplementary figure:

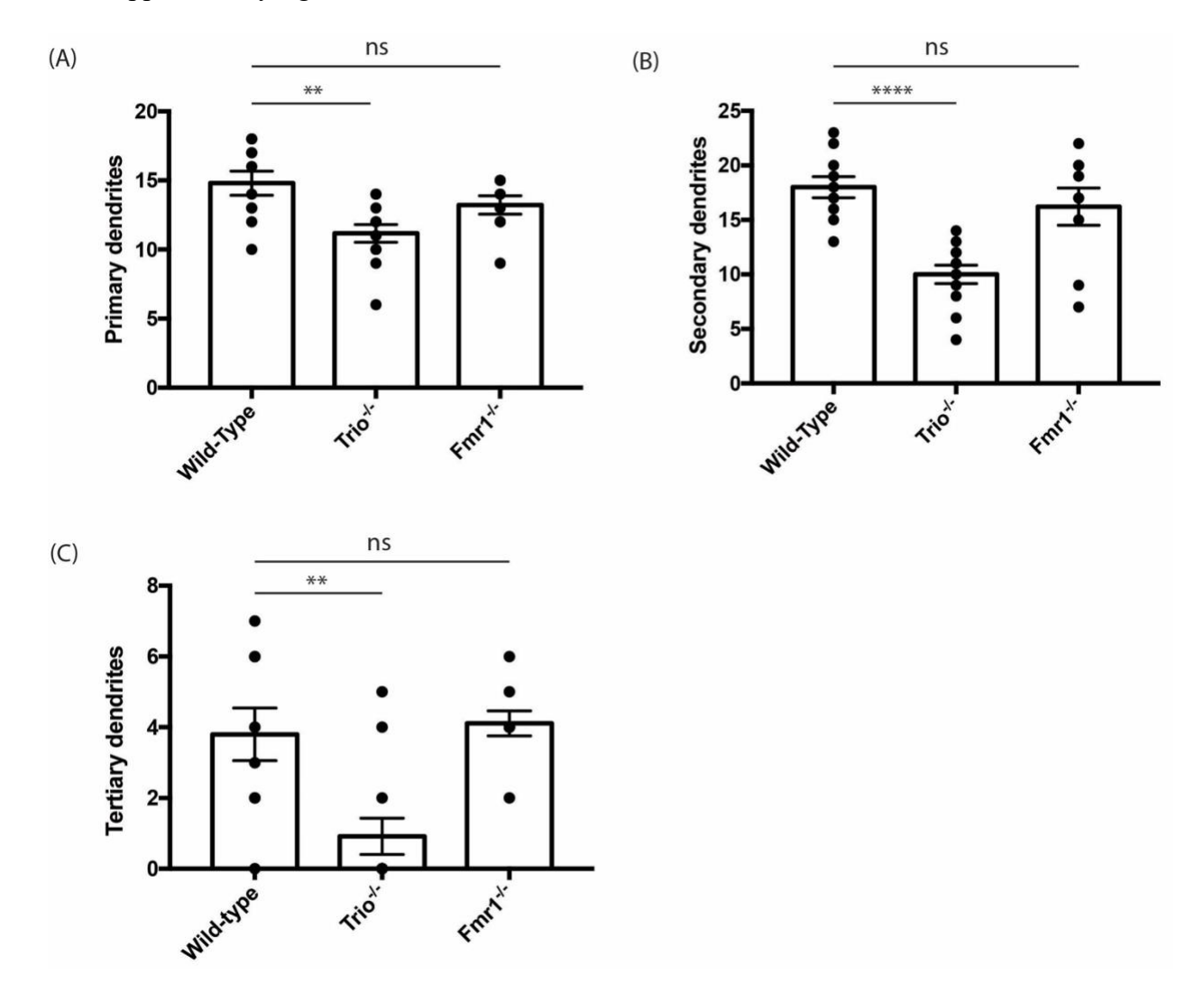


Figure 3 Supplementary 1: The number of dendrites for individual orders of branching. (A) There is a significant difference in the number of primary dendrites between WT and the Trio mutant. bu(B) The number of secondary dendrites is significantly lower in the Trio mutants as compared to the WT. (C) There is also a significant difference in the number of tertiary dendrites between the WT and the Trio mutant. However, there is no significant difference in any order of branching between the WT and the Fmr1 mutant.

#### 2.9. References:

Avila, A., Paculis, L., Tascon, R. G., Ramos, B., & Jia, D. (2024). A large-scale in vivo screen to investigte the roles of human genes in Drosophila melanogaster. *G3 (Bethesda, Md.)*, *14*(10), jkae188. <a href="https://doi.org/10.1093/g3journal/jkae188">https://doi.org/10.1093/g3journal/jkae188</a>

Awasaki, T., Saito, M., Sone, M., Suzuki, E., Sakai, R., Ito, K., & Hama, C. (2000). The Drosophila trio plays an essential role in patterning of axons by regulating their directional extension. *Neuron*, *26*(1), 119–131. https://doi.org/10.1016/s0896-6273(00)81143-5

Bagni, C., & Greenough, W. T. (2005). From mRNP trafficking to spine dysmorphogenesis: the roots of fragile X syndrome. *Nature reviews. Neuroscience*, *6*(5), 376–387. https://doi.org/10.1038/nrn1667

Banerjee, S., Venkatesan, A., & Bhat, M. A. (2017). Neurexin, Neuroligin and Wishful Thinking coordinate synaptic cytoarchitecture and growth at neuromuscular junctions.

\*Molecular and cellular neurosciences\*, 78, 9–24. <a href="https://doi.org/10.1016/j.mcn.2016.11.004">https://doi.org/10.1016/j.mcn.2016.11.004</a>

Bellen, H. J., Tong, C., & Tsuda, H. (2010). 100 years of Drosophila research and its impact on vertebrate neuroscience: a history lesson for the future. *Nature reviews. Neuroscience*, 11(7), 514–522. <a href="https://doi.org/10.1038/nrn2839">https://doi.org/10.1038/nrn2839</a>

Chen, K., Gracheva, E. O., Yu, S. C., Sheng, Q., Richmond, J., & Featherstone, D. E. (2010). Neurexin in embryonic Drosophila neuromuscular junctions. *PloS one*, *5*(6), e11115. https://doi.org/10.1371/journal.pone.0011115

Chmielewska, J. J., Kuzniewska, B., Milek, J., Urbanska, K., & Dziembowska, M. (2019). Neuroligin 1, 2, and 3 Regulation at the Synapse: FMRP-Dependent Translation and Activity-Induced Proteolytic Cleavage. *Molecular neurobiology*, *56*(4), 2741–2759. https://doi.org/10.1007/s12035-018-1243-1

Coulson, B., Hunter, I., Doran, S., Parkin, J., Landgraf, M., & Baines, R. A. (2022). Critical periods in *Drosophila* neural network development: Importance to network tuning and therapeutic potential. *Frontiers in physiology*, *13*, 1073307.

https://doi.org/10.3389/fphys.2022.1073307

Doll, C. A., & Broadie, K. (2014). Impaired activity-dependent neural circuit assembly and refinement in autism spectrum disorder genetic models. *Frontiers in cellular neuroscience*, 8, 30. <a href="https://doi.org/10.3389/fncel.2014.00030">https://doi.org/10.3389/fncel.2014.00030</a>

Garces, A., & Thor, S. (2006). Specification of Drosophila aCC motoneuron identity by a genetic cascade involving even-skipped, grain and zfh1. *Development*, 133(8), 1445-1455.

https://doi.org/10.1242/dev.02321

Gatto, C. L., & Broadie, K. (2011). Drosophila modeling of heritable neurodevelopmental disorders. *Current opinion in neurobiology*, *21*(6), 834–841.

https://doi.org/10.1016/j.conb.2011.04.009

Grueber, W. B., Jan, L. Y., & Jan, Y. N. (2002). Tiling of the Drosophila epidermis by multidendritic sensory neurons. *Development (Cambridge, England)*, *129*(12), 2867–2878. https://doi.org/10.1242/dev.129.12.2867

Guan, B., Hartmann, B., Kho, Y. H., Gorczyca, M., & Budnik, V. (1996). The Drosophila tumor suppressor gene, dlg, is involved in structural plasticity at a glutamatergic synapse.

Current biology: CB, 6(6), 695–706. https://doi.org/10.1016/s0960-9822(09)00451-5

Harris, K. P., & Littleton, J. T. (2015). Transmission, Development, and Plasticity of Synapses. *Genetics*, 201(2), 345–375. https://doi.org/10.1534/genetics.115.176529

Hunter, I., Coulson, B., Pettini, T., Davies, J. J., Parkin, J., Landgraf, M., & Baines, R. A. (2024). Balance of activity during a critical period tunes a developing network. *eLife*, *12*, RP91599. <a href="https://doi.org/10.7554/eLife.91599">https://doi.org/10.7554/eLife.91599</a>

Hutchinson, K. M., Vonhoff, F., & Duch, C. (2014). Dscam1 is required for normal dendrite growth and branching but not for dendritic spacing in Drosophila motoneurons. *The Journal of neuroscience : the official journal of the Society for Neuroscience*, *34*(5), 1924–1931. https://doi.org/10.1523/JNEUROSCI.3448-13.2014

Inal, M. A., Banzai, K., & Kamiyama, D. (2020). Retrograde Tracing of Drosophila Embryonic Motor Neurons Using Lipophilic Fluorescent Dyes. *J Vis Exp*(155). <a href="https://doi.org/10.3791/60716">https://doi.org/10.3791/60716</a> Inal, M. A., Banzai, K., Kamiyama, R., & Kamiyama, D. (2024). Cell-type-specific Labeling of Endogenous Proteins Using the Split GFP System in *Drosophila*. *bioRxiv*: *the preprint server for biology*, 2024.05.06.592806. <a href="https://doi.org/10.1101/2024.05.06.592806">https://doi.org/10.1101/2024.05.06.592806</a>

Irwin, S. A., Galvez, R., & Greenough, W. T. (2000). Dendritic spine structural anomalies in fragile-X mental retardation syndrome. *Cerebral cortex (New York, N.Y. : 1991)*, *10*(10), 1038–1044. <a href="https://doi.org/10.1093/cercor/10.10.1038">https://doi.org/10.1093/cercor/10.10.1038</a>

Iyer, S. C., Wang, D., Iyer, E. P., Trunnell, S. A., Meduri, R., Shinwari, R., Sulkowski, M. J., & Cox, D. N. (2012). The RhoGEF trio functions in sculpting class specific dendrite morphogenesis in Drosophila sensory neurons. *PloS one*, *7*(3), e33634. https://doi.org/10.1371/journal.pone.0033634

Jan, Y. N., & Jan, L. Y. (2010). Branching out: mechanisms of dendritic arborization. *Nature reviews. Neuroscience*, 11(5), 316–328. https://doi.org/10.1038/nrn2836

Jeibmann, A., & Paulus, W. (2009). Drosophila melanogaster as a model organism of brain diseases. *International journal of molecular sciences*, 10(2), 407–440. <a href="https://doi.org/10.3390/ijms10020407">https://doi.org/10.3390/ijms10020407</a> Kamiyama, D., McGorty, R., Kamiyama, R., Kim, M. D., Chiba, A., & Huang, B. (2015). Specification of Dendritogenesis Site in Drosophila aCC Motoneuron by Membrane Enrichment of Pak1 through Dscam1. *Developmental cell*, 35(1), 93–106.

Kamiyama, R., Banzai, K., Liu, P., Marar, A., Tamura, R., Jiang, F., Fitch, M. A., Xie, J., & Kamiyama, D. (2021). Cell-type-specific, multicolor labeling of endogenous proteins with split fluorescent protein tags in *Drosophila*. *Proceedings of the National Academy of Sciences of the United States of America*, 118(23), e2024690118.

https://doi.org/10.1073/pnas.2024690118

https://doi.org/10.1016/j.devcel.2015.09.007

Krueger, D. D., Tuffy, L. P., Papadopoulos, T., & Brose, N. (2012). The role of neurexins and neuroligins in the formation, maturation, and function of vertebrate synapses. *Current opinion in neurobiology*, 22(3), 412–422. <a href="https://doi.org/10.1016/j.conb.2012.02.012">https://doi.org/10.1016/j.conb.2012.02.012</a>

Kuehn, C., & Duch, C. (2013). Putative excitatory and putative inhibitory inputs are localised in different dendritic domains in a Drosophila flight motoneuron. *The European journal of neuroscience*, *37*(6), 860–875. <a href="https://doi.org/10.1111/ejn.12104">https://doi.org/10.1111/ejn.12104</a>

Lee, A., Li, W., Xu, K., Bogert, B. A., Su, K., & Gao, F. B. (2003). Control of dendritic development by the Drosophila fragile X-related gene involves the small GTPase Rac1.

Development (Cambridge, England), 130(22), 5543–5552. https://doi.org/10.1242/dev.00792

Li, H., & Gavis, E. R. (2022). The Drosophila fragile X mental retardation protein modulates the neuronal cytoskeleton to limit dendritic arborization. *Development (Cambridge, England)*, *149*(10), dev200379. <a href="https://doi.org/10.1242/dev.200379">https://doi.org/10.1242/dev.200379</a>

Li, Z., Van Aelst, L., & Cline, H. T. (2000). Rho GTPases regulate distinct aspects of dendritic arbor growth in Xenopus central neurons in vivo. *Nature neuroscience*, *3*(3), 217–225. https://doi.org/10.1038/72920

Mendoza, C., Olguín, P., Lafferte, G., Thomas, U., Ebitsch, S., Gundelfinger, E. D., Kukuljan, M., & Sierralta, J. (2003). Novel isoforms of Dlg are fundamental for neuronal development in Drosophila. *The Journal of neuroscience : the official journal of the Society for Neuroscience*, 23(6), 2093–2101. <a href="https://doi.org/10.1523/JNEUROSCI.23-06-02093.2003">https://doi.org/10.1523/JNEUROSCI.23-06-02093.2003</a>

Nguyen, T. A., Lehr, A. W., & Roche, K. W. (2020). Neuroligins and Neurodevelopmental Disorders: X-Linked Genetics. *Frontiers in synaptic neuroscience*, *12*, 33. <a href="https://doi.org/10.3389/fnsyn.2020.00033">https://doi.org/10.3389/fnsyn.2020.00033</a>

Pan, L., Zhang, Y. Q., Woodruff, E., & Broadie, K. (2004). The Drosophila fragile X gene negatively regulates neuronal elaboration and synaptic differentiation. *Current biology: CB*, 14(20), 1863–1870. <a href="https://doi.org/10.1016/j.cub.2004.09.085">https://doi.org/10.1016/j.cub.2004.09.085</a>

Parenti, I., Rabaneda, L. G., Schoen, H., & Novarino, G. (2020). Neurodevelopmental Disorders: From Genetics to Functional Pathways. *Trends in neurosciences*, *43*(8), 608–621. https://doi.org/10.1016/j.tins.2020.05.004 Parisi, M. J., Aimino, M. A., & Mosca, T. J. (2023). A conditional strategy for cell-type-specific labeling of endogenous excitatory synapses in *Drosophila*. *Cell reports methods*, 3(5), 100477. https://doi.org/10.1016/j.crmeth.2023.100477

Peng, Y. J., He, W. Q., Tang, J., Tao, T., Chen, C., Gao, Y. Q., Zhang, W. C., He, X. Y., Dai, Y. Y., Zhu, N. C., Lv, N., Zhang, C. H., Qiao, Y. N., Zhao, L. P., Gao, X., & Zhu, M. S. (2010). Trio is a key guanine nucleotide exchange factor coordinating regulation of the migration and morphogenesis of granule cells in the developing cerebellum. *The Journal of biological chemistry*, 285(32), 24834–24844. <a href="https://doi.org/10.1074/jbc.M109.096537">https://doi.org/10.1074/jbc.M109.096537</a>

Ryglewski, S., Vonhoff, F., Scheckel, K., & Duch, C. (2017). Intra-neuronal Competition for Synaptic Partners Conserves the Amount of Dendritic Building Material. *Neuron*, *93*(3), 632–645.e6. <a href="https://doi.org/10.1016/j.neuron.2016.12.043">https://doi.org/10.1016/j.neuron.2016.12.043</a>

Sánchez-Soriano, N., Bottenberg, W., Fiala, A., Haessler, U., Kerassoviti, A., Knust, E., Löhr, R., & Prokop, A. (2005). Are dendrites in Drosophila homologous to vertebrate dendrites?. *Developmental biology*, 288(1), 126–138.

https://doi.org/10.1016/j.ydbio.2005.09.026

Sanfilippo, P., Kim, A. J., Bhukel, A., Yoo, J., Mirshahidi, P. S., Pandey, V., Bevir, H., Yuen, A., Mirshahidi, P. S., Guo, P., Li, H. S., Wohlschlegel, J. A., Aso, Y., & Zipursky, S. L. (2024). Mapping of multiple neurotransmitter receptor subtypes and distinct protein complexes to the connectome. *Neuron*, *112*(6), 942–958.e13.

https://doi.org/10.1016/j.neuron.2023.12.014

Say, E., Tay, H. G., Zhao, Z. S., Baskaran, Y., Li, R., Lim, L., & Manser, E. (2010). A functional requirement for PAK1 binding to the KH(2) domain of the fragile X protein-related FXR1. *Molecular cell*, *38*(2), 236–249. <a href="https://doi.org/10.1016/j.molcel.2010.04.004">https://doi.org/10.1016/j.molcel.2010.04.004</a>
Scott, E. K., Reuter, J. E., & Luo, L. (2003). Small GTPase Cdc42 is required for multiple aspects of dendritic morphogenesis. *The Journal of neuroscience : the official journal of the Society for Neuroscience*, *23*(8), 3118–3123. <a href="https://doi.org/10.1523/JNEUROSCI.23-08-03118.2003">https://doi.org/10.1523/JNEUROSCI.23-08-03118.2003</a>

Seroka, A., Lai, S. L., & Doe, C. Q. (2022). Transcriptional profiling from whole embryos to single neuroblast lineages in Drosophila. *Developmental biology*, 489, 21–33.

https://doi.org/10.1016/j.ydbio.2022.05.018

Shivalkar, M., & Giniger, E. (2012). Control of dendritic morphogenesis by Trio in Drosophila melanogaster. *PloS one*, 7(3), e33737. <a href="https://doi.org/10.1371/journal.pone.0033737">https://doi.org/10.1371/journal.pone.0033737</a>
Stanko, J. P., Easterling, M. R., & Fenton, S. E. (2015). Application of Sholl analysis to quantify changes in growth and development in rat mammary gland whole mounts. *Reproductive toxicology (Elmsford, N.Y.)*, *54*, 129–135.

https://doi.org/10.1016/j.reprotox.2014.11.004

Stilwell, G. E., & ffrench-Constant, R. H. (1998). Transcriptional analysis of the Drosophila GABA receptor gene resistance to dieldrin. *Journal of neurobiology*, *36*(4), 468–484. https://doi.org/10.1002/(sici)1097-4695(19980915)36:4<468::aid-neu2>3.0.co;2-u

Venken, K. J., Simpson, J. H., & Bellen, H. J. (2011). Genetic manipulation of genes and cells in the nervous system of the fruit fly. *Neuron*, 72(2), 202–230.

https://doi.org/10.1016/j.neuron.2011.09.021

Washbourne P. (2015). Synapse assembly and neurodevelopmental disorders.

Neuropsychopharmacology: official publication of the American College of Neuropsychopharmacology, 40(1), 4–15. https://doi.org/10.1038/npp.2014.163

Zeng, X., Sun, M., Liu, L., Chen, F., Wei, L., & Xie, W. (2007). Neurexin-1 is required for synapse formation and larvae associative learning in Drosophila. *FEBS letters*, *581*(13), 2509–2516. https://doi.org/10.1016/j.febslet.2007.04.068

Zhang, X., Rui, M., Gan, G., Huang, C., Yi, J., Lv, H., & Xie, W. (2017). Neuroligin 4 regulates synaptic growth via the bone morphogenetic protein (BMP) signaling pathway at the *Drosophila* neuromuscular junction. *The Journal of biological chemistry*, 292(44), 17991–18005. https://doi.org/10.1074/jbc.M117.810242